# Plasmin-sensitive Dibasic Sequences in the Third Fibronectin-like Domain of L1–Cell Adhesion Molecule (CAM) Facilitate Homomultimerization and Concomitant Integrin Recruitment

**Steve Silletti,*‡ Fang Mei,‡ Dean Sheppard,§‖ and Anthony M.P. Montgomery*‡**

*Department of Pediatrics, University of California at San Diego, La Jolla, California 92037; ‡Department of Immunology, The Scripps Research Institute, La Jolla, California 92037; and §Lung Biology Center, Center for Occupational and Environmental Health, Cardiovascular Research Institute, ‖Department of Medicine, University of California, San Francisco, California 94080

*Abstract.* L1 is a multidomain transmembrane neural recognition molecule essential for neurohistogenesis. While moieties in the immunoglobulin-like domains of L1 have been implicated in both heterophilic and homophilic binding, the function of the fibronectin (FN)-like repeats remains largely unresolved. Here, we demonstrate that the third FN-like repeat of L1 (FN3) spontaneously homomultimerizes to form trimeric and higher order complexes. Remarkably, these complexes support direct RGD-independent interactions with several integrins, including $\alpha_v\beta_3$ and $\alpha_5\beta_1$. A peptide derived from the putative C-C′ loop of FN3 (GSQRKHSKRHIHKDHV$^{852}$) also forms trimeric complexes and supports $\alpha_v\beta_3$ and $\alpha_5\beta_1$ binding. Substitution of the dibasic RK$^{841}$ and KR$^{845}$ sequences within this peptide or the FN3 domain limited multimerization and abrogated integrin binding. Evidence is presented that the multimerization of, and integrin binding to, the FN3 domain is regulated both by conformational constraints imposed by other domains and by plasmin-mediated cleavage within the sequence RK$^{\downarrow}$HSK$^{\downarrow}$RH$^{846}$. The integrin $\alpha_9\beta_1$, which also recognizes the FN3 domain, colocalizes with L1 in a manner restricted to sites of cell–cell contact. We propose that distal receptor ligation events at the cell–cell interface may induce a conformational change within the L1 ectodomain that culminates in receptor multimerization and integrin recruitment via interaction with the FN3 domain.

Key words: neural CAM • heterophilic ligation • melanoma • $\alpha_v\beta_3$ • $\alpha_5\beta_1$ • $\alpha_9\beta_1$

## *Introduction*

Human L1 is a member of a subfamily of phylogenetically conserved neural recognition molecules that share a complex ectodomain structure consisting of multiple immunoglobulin and fibronectin (FN)[1] type III repeats (Hortsch, 1996). Orthologues of human and mouse L1 have been described, including NILE (rat), NgCAM (chick), E587 (goldfish), L1.1/L1.2 (zebrafish), and neuroglian (*Drosophila*) (Bock et al., 1985; Lemmon and McLoon, 1986; Bieber et al., 1989; Bastmeyer et al., 1995; Tongiorgi et al., 1995). Pioneering studies implicated the L1 subfamily in a variety of dynamic neurological processes, including neurite fasciculation and outgrowth, as well as cerebellar cell migration (Lindner et al., 1983; Martini and Schachner, 1986; Lagenaur and Lemmon, 1987). With the recent generation of L1-deficient mice, it has been confirmed that L1 is required for normal corticospinal axon guidance (Cohen et al., 1997) and for axonal ensheathment by nonmyelinating Schwann cells (Dahme et al., 1997; Haney et al., 1999). Many of the neuropathologies now described in L1 knockout mice, including dilated brain ventricles, abnormal dendritic architecture, and developmental defects in the hippocampus and corpus callosum (Dahme et al., 1997; Demyanenko et al., 1999), are consistent with the manifestations of CRASH, a neurological syndrome associated with mutations in the human L1 gene (Fransen et al., 1997; Brummendorf et al., 1998).

Although designated a neural cell adhesion molecule (CAM), both murine and human L1 homologues have been described on cells of diverse histological origin including epithelial cells associated with kidney collecting ducts (Debiec et al., 1998) and with the intestinal and urogenital tract (Thor et al., 1987; Kujat et al., 1995). Interest-

Address correspondence to Anthony Montgomery, Department of Pediatrics-0983, The Whittier Institute, University of California at San Diego, 9894 Genesee Avenue, La Jolla, CA 92037. Tel.: (858) 550-2909. Fax: (858) 558-3495. E-mail: ammontgo@ucsd.edu

[1]*Abbreviations used in this paper:* CAM, cell adhesion molecule; ECD, ectodomain; FN, fibronectin; pAb, polyclonal antibody; RGD, arginine-glycine-aspartate.

ingly, the L1 expressed by renal epithelium has been shown to be important for normal branching morphogenesis (Debiec et al., 1998). Cells of lymphoid and myelomonocytic origin also express L1 (Ebeling et al., 1996; Pancook et al., 1997), however, the functional significance of L1 within the immune system remains to be determined. In this regard, Di Sciullo et al. (1998) have shown that L1 is important for maintaining normal lymph node architecture during an immune response and suggest a mechanism based on the expression of L1 by reticular fibroblasts. A potential function for L1 in tumor progression is also suggested by widespread expression on many tumor cell lines including neuroectodermal tumors (melanoma and neuroblastoma), carcinomas (lung, renal, and skin), and monocytic leukemias (Mujoo et al., 1986; Linnemann et al., 1989; Reid and Hemperly, 1992; Katayama et al., 1997; Pancook et al., 1997). Supporting a role for L1 in tumor progression, Linnemann et al. (1989) reported finding elevated levels of L1 on a metastatic variant of a melanoma cell line. Indeed, a recent study by Ohnishi et al. (1998) suggests that L1 may promote metastasis by facilitating tumor cell invasion or migration.

Structure–function studies have defined multiple interactive moieties within L1 that facilitate either homophilic or heterophilic interactions (Hortsch, 1996). Thus far, many of the interactions defined involve one or more of the six Ig-like domains that constitute the $NH_2$-terminal portion of the L1 ectodomain. An antiparallel alignment of the first four Ig-like domains of L1 is proposed to facilitate homophilic L1–L1 binding (Su et al., 1998). The chondroitin sulfate proteoglycan, neurocan, binds with high affinity to the $NH_2$-terminal Ig-like domain of L1 (Oleszewski et al., 1999). An arginine-glycine-aspartate (RGD) motif in the sixth Ig-like domain of human L1 supports heterophilic interactions with multiple members of the integrin superfamily, including $\alpha_v\beta_3$ and $\alpha_5\beta_1$ (Montgomery et al., 1996; Felding-Habermann et al., 1997; Oleszewski et al., 1999). Axonin-1/TAG-1, a neuron-specific CAM, undergoes a cis-interaction with the chick L1-orthologue NgCAM via multiple moieties including the first and second Ig-like domains as well as the third FN-like repeat (Kunz et al., 1998). Other cis-interacting elements include the tetraspan signaling molecule CD9 (Schmidt et al., 1996), NCAM (Feizi, 1994), and the heat-stable antigen CD24 (Kadmon et al., 1995), although the regions of L1 responsible for these interactions have yet to be determined.

The functional significance of the FN-like repeats that constitute the membrane-proximal portion of the L1 ectodomain remains largely unresolved. An antibody directed to an epitope between FN-like repeats 2 and 3 has been shown to promote signal transduction and concomitant neurite extension (Appel et al., 1995). Based on this observation the authors proposed that distal recognition events may induce conformational changes that are funneled to a region within the FN-like repeats, which then represents the ultimate site for the induction of signaling events. Recent rotary shadow analysis of the purified L1 ectodomain showed that the FN-like repeats assume a tight globular configuration (Drescher et al., 1996). Any conformational lability within this structure may, therefore, provide a mechanism for translating distal ligation events into signaling events. In a further study, Holm et al. (1995) demonstrated that certain FN-like domain fragments have a capacity for homoaggregation, suggesting that one or more of the FN-like domains may have the potential for self-association, perhaps leading to the clustering of L1 at the cell surface; such clustering may in turn be subject to conformational constraints imposed by the globular configuration of the FN-like repeats.

In this study, we have identified moieties within the third FN-like repeat of L1 (FN3) that can simultaneously potentiate receptor clustering and integrin recruitment. Both multimerization of, and integrin binding to, the FN3 domain are shown to be critically regulated by conformational constraints imposed by other domains and by proteolysis. Several integrins are implicated in binding to the FN3 domain including $\alpha_v\beta_3$, $\alpha_5\beta_1$, and $\alpha_9\beta_1$. Based on our findings, we propose that ligation events at the cell–cell interface may induce a conformation change within the L1 ectodomain that culminates in receptor multimerization and integrin recruitment via the FN3 domain. This paradigm has important implications for L1 signaling and for the modulation of integrin activity during cell–cell interactions.

## *Materials and Methods*

### *Reagents*

Antiintegrin antibodies used in this study include the following: anti-$\beta_1$ mAbs P4C10, LM534, B44, and Cl. 18; anti-$\alpha_5\beta_1$ mAbs P1D6 and NKI-SAM-1, anti-$\alpha_5$ mAb Cl.1, anti-$\alpha_9\beta_1$ mAb Y9A2; anti-$\alpha_v\beta_3$ mAb LM609; anti-$\beta_3$ antibody AP3; anti-$\beta_5$ antibody 11D1; and an anti-$\alpha_v$/anti-$\beta_3$ (anti-VNR) polyclonal antibody (pAb). mAbs B44, P1D6, and Y9A2 were purchased from Chemicon International. mAbs Cl. 18 and Cl.1 were purchased from Transduction Laboratories. mAb NKI-SAM-1 was purchased from Southern Biotechnology. mAb P4C10 was provided by Dr. E.A. Wayner (University of Minnesota, Minneapolis, MN). LM609, the anti–human L1 mAb 5G3 (Mujoo et al., 1986), the anti–L1-Ig6 mAb LP1B9, the anti-VNR pAb, and the anti-5G3 Ag pAb were generated within the Scripps Research Institute. Antibodies AP3 and 11D1 were provided by Dr. David Cheresh (The Scripps Research Institute). An anti–L1 ectodomain (anti–L1-ECD) pAb was generated against, and affinity-purified using the L1 ectodomain fusion protein. A pAb specific for glutathione S-transferase (GST) was purchased from Upstate Biotechnology Inc. L1 peptides were synthesized on an ABI 430A peptide synthesizer within The Scripps Research Institute Core Facility as described previously (Felding-Habermann et al., 1997). For the purpose of immobilization, most peptides were made with $NH_2$-terminal cysteine residues. RGD and RGE control peptides were as follows: GRGDSPC and GRGESPC. Human plasmin was purchased from Calbiochem.

### *Cell Lines and Culture*

M21 human melanoma cells were derived from the UCLA-SO-M21 cell line, which was provided by Dr. D.L. Morton (University of California, Los Angeles, CA). Variant αv-integrin–deficient cells (M21-L) were negatively selected from M21 cells by FACS at The Scripps Research Institute. All cells were maintained in RPMI-1640 supplemented with 10% FCS. Transfected CHO cells bearing the human $\alpha_9$ integrin subunit were generated in the laboratory of Dr. Sheppard and cultured as described (Taooka et al., 1999).

### *Construction and Expression of L1 Fusion Proteins*

The recombinant L1 fusion proteins shown in Table I (schematic) were generated by PCR amplification of appropriate coding sequences and restriction cloned into the appropriate fusion vector based upon the required tag and reading frame. Primer sequences and their corresponding L1 amino acid start (sense oligos) or stop (antisense oligos) translation

*Table I. Oligonucleotide Primers Used in the Construction of Recombinant L1 Domains*

| Primer | L1 Coding Sequence | Oligonucleotide Sequence |
|---|---|---|
| PCR | | |
| Ig6 Sense | Start at 499 (EcoRI) | 5'-AAAGAATTCACTCAGATCACT-3' |
| Ig6 Antisense | Stop at 595 (EcoRI) | 5'-CGTGAATTCGGCCCAGGGCTC-3' |
| FN1 Sense | Start at 593 (BamHI) | 5'-GTGGGATCCCCTGGGCCGGTGC-3' |
| FN1 Antisense | Stop at 697 (EcoRI) | 5'-TGAATTCTTCTCTGGGGCTGCC-3' |
| FN2 Sense | Start at 700 (EcoRI) | 5'-AGAATTCTGTGGATGTGAAGGGGG-3' |
| FN2 Antisense | Stop at 795 (EcoRI) | 5'-GGAATTCCCTGGGGGTAGTC-3' |
| FN3 Sense | Start at 792 (EcoRI) | 5'-GGAGAATTCTACCCCCAGGCA-3' |
| FN3 Antisense | Stop at 903 (EcoRI) | 5'-GGAATTCCTCGGGGTGGCCAG-3' |
| Mutagenesis | | |
| K/A Sense | K823A | 5'-CCGGTGGACCTGGCCCAAGTCGCAGGACACCTCCGCGGATACAAT-3' |
| K/A Antisense | | 5'-ATTGTATCCGCGGAGGTGTCCTGCGACTTGGGCCAGGTCCACCGG-3' |
| 2XN Sense | KR844/45NN | 5'-GAGGAAGCACAGCAATAATCATATCCACAAAGACC-3' |
| 2XN Antisense | | 5'-GGTCTTTGTGGATATGATTATTGCTGTGCTTCCTC-3' |
| 4XN Sense* | RKKR840/41/44/45NNNN | 5'-TGGAGGGAGGGCAGTCAGAATAATCACAGCAATAATCATATC-3' |
| 4XN Antisense* | | 5'-GATATGATTATTGCTGTGATTATTCTGACTGCCCTCCCTCCA-3' |
| | | *4XN was generated using the 2XN construct as template |

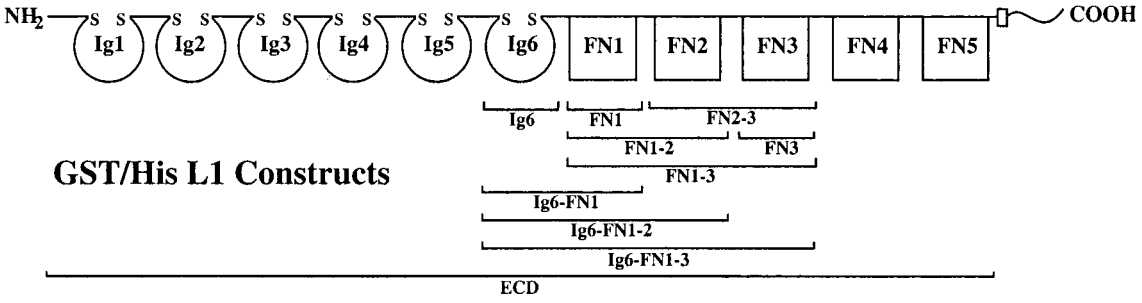


Underlined bases represent sequences responsible for mutations in mutagenesis primers and restriction sites in PCR primers.

sites, as well as the restriction enzymes used for insertion of the respective PCR products into the respective fusion protein vectors, are shown in Table I. Plasmids were purchased from Amersham Pharmacia Biotech or GIBCO BRL for pGEX GST fusion vectors or pProEX 6×His fusion vectors, respectively. Mutagenesis of the FN3 construct was performed essentially as described previously (Nayeem et al., 1999). In brief, mutagenic sense and antisense oligonucleotides (Table I) were annealed and extended with *Pfu* polymerase for a total of 18 cycles. Nonmutant starting material was digested with DpnI and the final product was transformed into supercompetent *Escherichia coli*. Final constructs were confirmed by dideoxy sequencing.

Purification of the recombinant fusion proteins was performed from log phase BL21 strain *E. coli* induced with either 100 μM (GST) or 600 μM isopropyl-β-D-thiogalactopyranoside (6×His). GST fusion protein purification was performed as previously described (Nayeem et al., 1999). For His fusion protein purification, cultures were resuspended in lysis buffer (50 mM Tris-HCl, pH 8.5, 300 mM KCl, 20 mM imidazole, and 0.1% Triton X-100–containing protease inhibitors) and incubated with 100 μg/ml lysozyme at 4°C. Lysates were clarified by centrifugation and fusion proteins were immobilized on Ni-NTA agarose (Qiagen) before extensive washing of the matrix with lysis buffer, followed by washing with 50 mM Tris-HCl, pH 8.5, 500 mM KCl, 40 mM imidazole, and elution with 20 mM Tris-HCl, pH 8.5, 300 mM KCl, 250 mM imidazole. Purified GST and His fusion proteins were dialyzed extensively against PBS.

## *Adhesion Assays*

Adhesion assays were performed essentially as described previously (Felding-Habermann et al., 1997). In brief, purified L1 fusion proteins (100–250 nM) were spotted (2-μl spots) or coated (100 μl) onto the bottom of 96-well Titertek plates (ICN Biomedicals) and allowed to coat for 1–2 h at 37°C before blocking with 5% BSA. For adhesion studies involving immobilized peptides, wells were precoated overnight with murine IgG2a antibody before incubation with the heterobifunctional cross-linker SPDP (Pierce Chemical Co.), washing and incubation with peptides at 100–200 μg/ml for 2–3 h before blocking with 5% BSA. Control wells received antibody and SPDP alone without peptide. Cells were harvested and resuspended in adhesion buffer (HBSS, 10 mM Hepes, 0.5% BSA, pH 7.4) containing divalent cations (0.4 mM $MnCl_2$, 1 mM $MgCl_2$, 1 mM $CaCl_2$) with or without antiintegrin function-blocking antibodies. For assays with $\alpha_v(-)$M21-L cells, adhesion was determined in the presence of 0.4 mM $MnCl_2$ alone. Cells were added at $10^5$ cells/well in the presence or absence of antibodies, and the plates were spun at 700 rpm to give a continuous monolayer. After 15–40 min at 37°C wells were washed with PBS, and the remaining adherent cells were fixed with 1% paraformaldehyde before counting the number of cells per high power field using a 40× objective and an ocular grid at a minimum of four areas per well. Experimental treatments were performed in triplicate.

## *Fractionation and Detection of L1-His Fusion Proteins*

L1-FN3 (His) fusion proteins (5 μg) were fractionated at a flow rate of 0.180 ml/min using a 40-ml bed volume Sephacryl S-200 column (Amersham Pharmacia Biotech). Fractions of 250 μl were collected, and 100 μl of each fraction was applied per well of a Ni-NTA HisSorb plate (Qiagen) for overnight immobilization at 4°C. Wells were subsequently washed with 0.5% BSA in PBS (BSA/PBS) before detection of bound His fusion protein as follows. Wells were incubated with anti–L1-ECD pAb for 1 h with

constant shaking before being washed at least five times with BSA/PBS and subsequently incubated with HRP-conjugated goat anti–rabbit secondary antibody (Jackson ImmunoResearch Laboratories). Wells were washed further and bound antibody was detected colorimetrically with TMB (Bio-Rad Laboratories). Color development was arrested with $H_2SO_4$, and the plates were read at 450 nm on a microplate reader (Kinetic Microplate Reader; Molecular Devices).

### *Integrin-binding Assays*

Purified $\alpha_v\beta_3$ and $\alpha_5\beta_1$ integrin heterodimers were purchased from Chemicon International. Integrin $\alpha_v\beta_3$ was biotinylated using NHS-LC-biotin (Pierce Chemical Co.). L1 fusion proteins (10–40 μg/ml) were adsorbed overnight at 4°C onto 96-well Titertek plates. Alternatively, 20 μg/ml of rabbit Ig was adsorbed before incubation with SPDP and immobilization of various peptides as described above for adhesion assays. After coating, the wells were washed and blocked with 0.5% BSA in TBS buffer. Purified integrin heterodimers were added at 1 μg/ml in TBS supplemented with 0.4 mM $MnCl_2$ and 0.5% BSA. After washing, bound $\alpha_v\beta_3$ was detected with an HRP-conjugated antibiotin mAb (Sigma Chemical Co.). Bound $\alpha_5\beta_1$ was detected with anti-$\alpha_5\beta_1$ mAb NKI-SAM-1, followed by HRP-conjugated goat anti–mouse Ig (Jackson ImmunoResearch Laboratories). Color was developed with TMB or OPD (Sigma Chemical Co.) and plates were read at 450 nm. Control wells received no integrin or were not coated with the L1 fusion protein. To assess the equivalent coating of immobilized GST fusion proteins, parallel wells were blocked with BSA/PBS, incubated with an anti-GST pAb, washed further, and incubated with an HRP-conjugated goat anti–rabbit antibody before colorimetric detection with either TMB or OPD at 450 nm.

### *Double Immunofluorescence*

Aggregated nonadherent $\alpha_v(-)$M21-L melanoma cells from routine tissue culture were harvested, washed, and resuspended in ice-cold FACS buffer (BSA/PBS with 0.05% $NaN_3$) for incubation with both anti-$\alpha_9\beta_1$ mAb Y9A2 and the anti–L1-ECD pAb. Cell aggregates were washed and double stained with fluorochrome-conjugated affinity-purified donkey F(ab′)-specific for mouse IgG (Texas red) or rabbit IgG (FITC), which had been preadsorbed to minimize cross-reactivity (Jackson ImmunoResearch Laboratories). Stained cell aggregates were mounted and analyzed using an MRC 1024 confocal microscope (Bio-Rad Laboratories) or a Nikon Eclipse E800 fluorescent microscope. Some stained cell aggregates were gently disrupted by pipetting in the presence of 1% paraformaldehyde, and single cells were assessed for L1 and $\alpha_9\beta_1$ colocalization. In further studies, all of the experimental steps described above were performed at 37°C in the absence of sodium azide.

### *Immunoprecipitation*

For analysis of the coprecipitation of L1 with integrin $\alpha_9\beta_1$, $\alpha_v(-)$M21-L cells were cultured until the nonadherent fraction contained numerous aggregates, at which time the adherent population was composed largely of independent cells. The nonadherent population was harvested, washed, and lysed in 50 mM Tris 7.6, 300 mM NaCl, 0.5% Triton X-100–containing protease inhibitors. Adherent cells were washed and lysed on the plate, and both adherent and nonadherent samples were clarified of Triton-insoluble material. Equal quantities of adherent and nonadherent cell lysate (3.5 mg) were precleared with protein G–Sepharose (Pierce Chemical Co.) before overnight incubation with 5 μg anti-$\alpha_9\beta_1$ mAb Y9A2. Antibody–antigen complexes were precipitated with protein G–Sepharose, washed with lysis buffer, and boiled in reducing SDS-PAGE sample buffer before being subjected to SDS-PAGE and immunoblotting with an anti–L1-ECD pAb and a combination of anti–$\beta_1$ integrin mAbs B44 and Cl. 18 as described below.

For studies on the coimmunoprecipitation of integrin subunits with L1, M21 or M21-L cells were aggregated by rotation, harvested, allowed to settle, and lysed as described above for the nonadherent M21-L population. After clarification of the Triton-insoluble fraction, equal quantities of lysate (7.5 mg) were precleared with protein A–Sepharose (Sigma Chemical Co.) before overnight incubation with 15 μg of either anti-5G3Ag pAb or a control anti-GST pAb. Antibody–antigen complexes were precipitated with protein A–Sepharose and washed extensively with lysis buffer (M21-L cells) or RIPA buffer (M21 cells) before boiling in nonreducing SDS-PAGE buffer and separation by SDS-PAGE and immunoblotting as described below. Precipitated L1 and associated integrins were detected with the appropriate antibody as follows: L1, mAb 5G3; $\beta_1$ integrin, mAb LM534; integrin $\alpha_5$, mAb Cl. 1; integrin $\beta_3$, mAb AP3; integrin $\beta_5$, mAb 11D1.

### *SDS-PAGE and Immunoblotting*

Peptides, purified proteins, or immunoprecipitates were prepared as described and separated in the presence or absence of 2-mercaptoethanol (as required) by SDS-PAGE on precast Tris-glycine gels (Novex). Separated proteins were electroblotted as required to a PVDF membrane (Immobilon-P; Millipore), which was subsequently blocked with 5% milk in PBS. Appropriate primary antibodies were incubated for 1–2 h in TBS containing 0.1% Tween 20 (TBS-T) and 0.5% milk, and bound primary antibody was detected with either an HRP-conjugated goat anti–rabbit Ig (Southern Biotechnology) or donkey anti–mouse Ig (Jackson ImmunoResearch Laboratories) preadsorbed to minimize cross-reactivity with the precipitating immunoglobulins. Antibody complexes were visualized with the chemiluminescent substrate PS-3 (Lumigen Inc.). Alternatively, gels were fixed and processed for staining.

## *Results*

### *The Third FN-like Repeat of L1 Promotes RGD-independent β1 Integrin Interaction with the L1 Ectodomain*

Previously, we have shown that the single RGD motif in the sixth Ig-like domain (Ig6) of human L1 is recognized by multiple integrin heterodimers, with the contribution of each of these integrins being dictated by cell type and the cation environment (Felding-Habermann et al., 1997). In a physiological cation environment, the adhesion of M21 melanoma cells to the Ig6 domain was found to be solely dependent on integrin $\alpha_v\beta_3$ (Montgomery et al., 1996). While these studies established the importance of the RGD motif in the context of individual domain fragments, integrin recognition of the intact L1 ectodomain was not addressed.

Significant dose-dependent adhesion of M21 cells was observed on immobilized fusion proteins consisting of either the Ig6 domain alone or the entire L1 ectodomain (Fig. 1 a). However, inhibition studies using function-blocking antibodies to either $\alpha_v\beta_3$ or $\beta_1$ integrin demonstrated a significant disparity in the contribution of these integrins to adhesion on the two substrates (Fig. 1 b). Thus, blocking ligation by $\alpha_v\beta_3$ resulted in a complete abrogation of adhesion to Ig6, but was only partially effective when the entire L1 ectodomain was used as a substrate (Fig. 1 b). This disparity can be attributed to supplemental $\beta_1$ integrin recognition of the L1 ectodomain, as adhesion to the L1 ectodomain could only be fully blocked with a combination of antibodies to both $\alpha_v\beta_3$ and $\beta_1$ integrins (Fig. 1 b; right).

These findings indicate that recognition of the RGD motif in L1-Ig6 can only partially account for the full measure of integrin binding to the entire L1 ectodomain. One possible explanation for this disparity is the presence of a second non-RGD motif recognized by one or more $\beta_1$ integrins. To identify the location of this motif, we generated multidomain L1 fragments containing the Ig6 domain and adjacent FN-like repeats. While the addition of the first and second proximal FN-like repeats of L1 (Ig6-FN1-2) failed to result in supplemental $\beta_1$ integrin binding (Fig. 1 c, left) inclusion of the third FN-like repeat (Ig6-FN1-3) did result in adhesion by both $\alpha_v\beta_3$ and $\beta_1$ integrin(s) (Fig. 1 c, right). These data indicate that recognition of sites

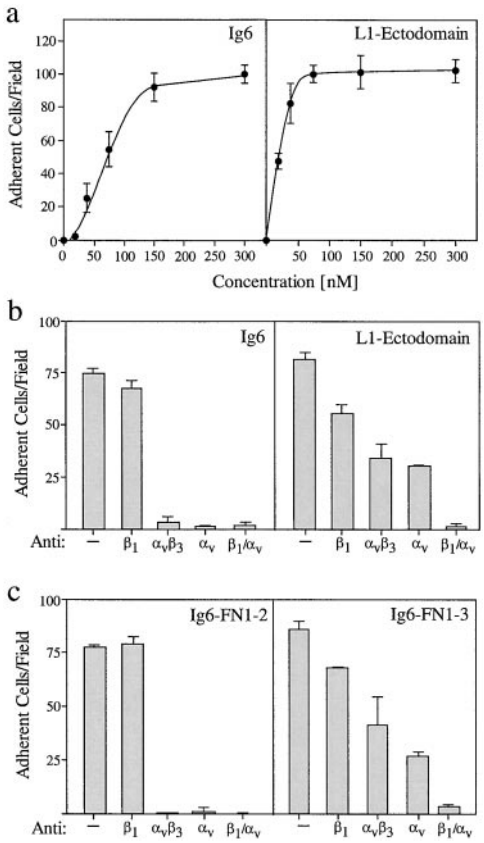


*Figure 1.* RGD-independent $\beta_1$ integrin binding to the L1 ectodomain involves the third FN-like repeat. (a) Adhesion of M21 cells to immobilized L1 ectodomain or domain Ig6 alone. (b) M21 adhesion to L1 ectodomain or Ig6 in the presence or absence of function-blocking antibody to $\alpha_v\beta_3$ (LM609), $\beta_1$ integrins (P4C10), $\alpha_v$ integrins (anti-VNR), or both $\alpha_v$ and $\beta_1$ integrins. (c) M21 adhesion to Ig6 with adjacent FN-like repeats (Ig6-FN1-2 and Ig6-FN1-3) in the presence or absence of function-blocking antibodies. Data shown is the mean of triplicate measurements ± SD.

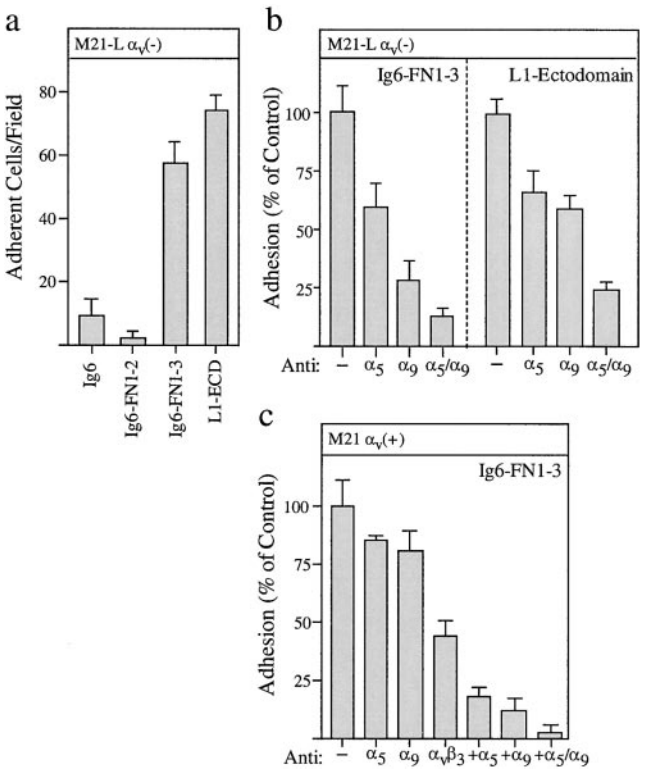


*Figure 2.* The third FN-like repeat of L1 is recognized by integrins $\alpha_5\beta_1$ and $\alpha_9\beta_1$. (a) Adhesion of $\alpha_v(-)$M21-L cells to immobilized L1 ectodomain, the Ig6 domain alone, or Ig6 in conjunction with adjacent FN-like repeats (Ig6-FN1-2 and Ig6-FN1-3). (b and c) Adhesion of $\alpha_v(-)$M21-L (b) or M21 cells (c) to L1 ectodomain or Ig6-FN1-3 in the presence or absence of function-blocking antibody to $\alpha_v\beta_3$ (LM609), $\alpha_5\beta_1$ (P1D6), or $\alpha_9\beta_1$ (Y9A2), alone or in combination. Data shown are the mean of triplicate measurements ± SD.

within Ig6 (RGD) and the third FN-like repeat (FN3; non-RGD), can fully account for integrin binding to the L1 ectodomain. It should be noted that the Ig-like domains proximal to Ig6 (i.e., Ig5 and Ig4) had no influence on integrin recognition (data not shown).

### *The Heterodimers $\alpha_5\beta_1$ and $\alpha_9\beta_1$ Are Responsible for $\beta_1$ Recognition of the Third FN-like Repeat of L1*

A panel of antiintegrin antibodies was tested to identify the $\beta_1$ integrin(s) responsible for recognition of the L1 ectodomain. These antibodies were first tested in adhesion assays using M21 cells selected for a lack of $\alpha_v$ integrin expression (i.e., M21-L cells). Because of the absence of $\alpha_v\beta_3$ expression, M21-L cell adhesion to L1-Ig6 or L1-Ig6-FN1-2 was minimal (Fig. 2 a). Consistent with $\beta_1$ integrin recognition of the third FN-like repeat, a marked increase in adhesion was observed on either Ig6-FN1-3 or on the L1 ectodomain (Fig. 2 a). Adhesion of $\alpha_v(-)$M21-L cells to both of these substrates was examined in the presence of function-blocking antibodies to a variety of $\beta_1$ integrins including $\alpha_1\beta_1$, $\alpha_2\beta_1$, $\alpha_3\beta_1$, $\alpha_4\beta_1$, $\alpha_5\beta_1$, $\alpha_6\beta_1$, and $\alpha_9\beta_1$. From these studies, it was confirmed that adhesion could only be abrogated using a combination of mAbs specific for both $\alpha_5\beta_1$ and $\alpha_9\beta_1$ (Fig. 2 b). Results obtained with the $\alpha_v(-)$M21-L cells could be reproduced with wild-type M21 cells provided $\alpha_v\beta_3$ binding by these cells was also blocked (Fig. 2 c). It should be noted that whereas wild-type M21 cells were able to utilize $\alpha_5\beta_1$ and $\alpha_9\beta_1$ for adhesion in a physiological cation environment (i.e., 1 mM $Ca^{2+}$, 1 mM $Mg^{2+}$, 0.4 mM $Mn^{2+}$), $\alpha_v(-)$M21-L cells only showed significant adhesion via these integrins in an activating cation environment consisting of 0.4 mM $Mn^{2+}$ alone. This unexpected finding suggests that the selection of M21 cells lacking $\alpha_v$ integrin expression has had an unforeseen effect on the activation state of these $\beta_1$ integrins.

### *The Third FN-like Repeat (FN3) Alone Supports Integrin Ligation But Recognition of This Domain Is Regulated by Upstream FN1*

To confirm that a second integrin recognition motif is present in the FN3 repeat, we generated a further series of L1 domain fragments consisting of single or multiple FN-like repeats, including FN3 alone as well as FN2-3 and FN1-3. L1 domain fragments consisting of FN1 alone and FN1-2 were generated as controls.

M21 cells failed to adhere to either FN1 or FN1-2, but

did display significant dose-dependent adhesion to the FN3 domain alone (Fig. 3 a). These findings confirm the importance of FN3 in adhesion and demonstrate that this domain can support adhesion independent of the RGD motif in Ig6. However, it is important to note that adhesion to FN3 was markedly reduced when this domain was offered together with both FN1 and FN2 domains (Fig. 3 a, FN1-3). This effect can be attributed to the presence of the first FN repeat (FN1) since adhesion to FN2-3 did not differ markedly from adhesion to FN3 alone (Fig. 3 a). Several explanations could account for the disparity in adhesion observed between the FN3 and FN1-3 domain constructs, including unequal adsorption of the GST fusion proteins. To exclude this possibility, we assessed the relative coating efficiency of the FN domain constructs by measuring the amount of immobilized GST present in coated wells. When offered at slightly different concentrations, which resulted in equalization of GST immunoreactivity (Fig. 3 b, inset), the significant disparity in adhesion between FN3 and FN1-3 was still observed, even though relatively high amounts of fusion protein were offered (Fig. 3 b). It is important to note that cell spreading was also markedly reduced on FN1-3, and that at lower coating concentrations, the disparity in adhesion between FN3 and FN1-3 was even more marked (Fig. 3 a). A further explanation for this reduced adhesion associated with the presence of FN1 would be an interaction between this domain and a cellular ligand that negatively regulates integrin ligation. However, it should be noted that FN1 did not impact integrin-mediated adhesion to Ig6. Thus, adhesion to a construct consisting of Ig6 and FN1 was not significantly different from that to Ig6 alone (Fig. 3 c).

To confirm that the adhesion observed with the FN3 domain alone is due to ligation of $\alpha_5\beta_1$ and $\alpha_9\beta_1$, further inhibition studies were performed with both M21 and $\alpha_v(-)$M21-L cells. As expected, $\alpha_v(-)$M21-L cell adhesion to both FN3 and FN1-3 was reduced by function-blocking antibodies to both $\alpha_5\beta_1$ and $\alpha_9\beta_1$ (Fig. 4 a). Wild-type M21

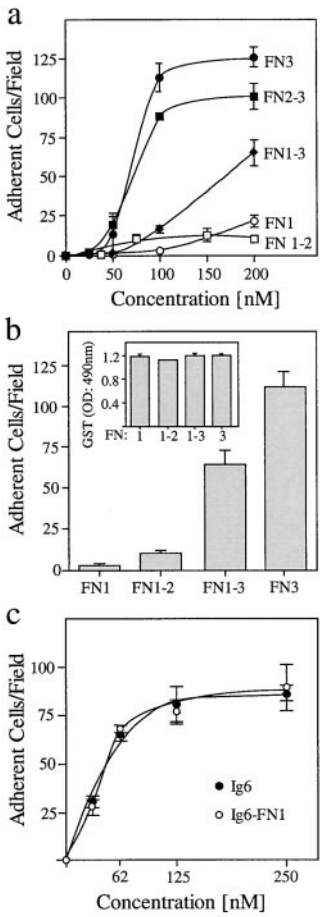


*Figure 3.* Adhesion to the third FN-like repeat of L1 (FN3) is regulated by the first FN-like repeat (FN1). (a) M21 adhesion to immobilized single domain fragments (FN1 and FN3) and multiple domain fragments (FN1-2, FN1-3, and FN2-3). (b) M21 adhesion to the immobilized FN domain fragments after equalizing for protein adsorption as determined by ELISA detection of GST (b, inset). (c) Adhesion of M21 cells to immobilized Ig6 or Ig6-FN1. Data shown are the mean of triplicate measurements ± SD.

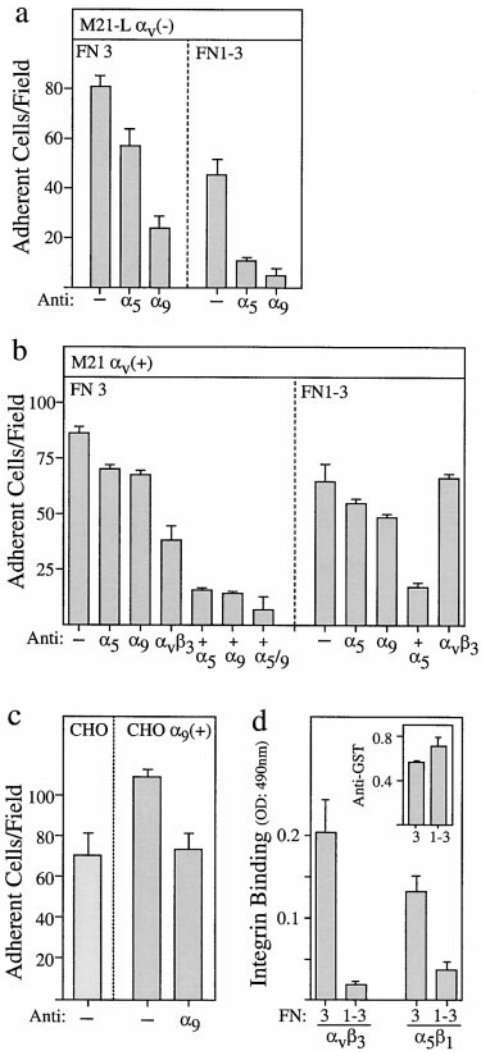


*Figure 4.* The FN3 domain alone is recognized by $\alpha_v\beta_3$ as well as $\alpha_5\beta_1$ and $\alpha_9\beta_1$, but this interaction is markedly inhibited by the FN1 domain. (a) Adhesion of $\alpha_v(-)$M21-L cells to immobilized FN3 alone or FN3 with the adjacent first and second FN-like domains (FN1-3) in the presence or absence of function-blocking antibodies to $\alpha_5\beta_1$ (P1D6) or $\alpha_9\beta_1$ (Y9A2). (b) Adhesion of M21 cells to immobilized FN 3 or FN1-3 in the presence or absence of function blocking antibody to $\alpha_v\beta_3$ (LM609), $\alpha_5\beta_1$ (P1D6), or $\alpha_9\beta_1$ (Y9A2), alone or in combination. (c) Mock-transfected CHO cells were compared with CHO cells transfected with the human integrin $\alpha_9$ subunit in the presence or absence of function-blocking antibody to $\alpha_9\beta_1$ (Y9A2). (d) Direct binding of purified $\alpha_v\beta_3$ or $\alpha_5\beta_1$ integrins to immobilized FN 3 or FN1-3 as determined by ELISA. The relative coating efficiency of the constructs was determined by anti-GST ELISA (inset). Data shown are the mean of triplicate measurements ± SD.

cell adhesion to FN1-3 was similarly abrogated using a combination of antibodies to $\alpha_5\beta_1$ and $\alpha_9\beta_1$ (Fig. 4 b, right). Remarkably, and in contrast to adhesion on FN1-3, M21 cell adhesion to FN3 could only be completely abrogated with the further addition of an antibody to $\alpha_v\beta_3$ (Fig. 4 b, left). These findings suggest that part of the antiadhesive activity of FN1 can be attributed to its capacity to significantly limit recognition of FN3 by $\alpha_v\beta_3$. However, since the adhesion of $\alpha_v(-)$M21-L cells was also reduced in the presence of FN1 (Fig. 4 a), it is likely that this domain also limits recognition by $\alpha_5\beta_1$ and $\alpha_9\beta_1$. To further establish that $\alpha_9\beta_1$ can directly support adhesion on FN3, it was determined that CHO cells transfected with the $\alpha_9$ subunit (Taooka et al., 1999) are significantly more adherent on FN3 than mock transfectants, and that the increased adhesion observed can be inhibited with a function-blocking antibody to $\alpha_9\beta_1$ (Fig. 4 c).

To confirm direct integrin binding to FN3 and to demonstrate regulation of this interaction by FN1, we performed binding assays with purified $\alpha_5\beta_1$ and $\alpha_v\beta_3$ heterodimers. The binding of these integrins to FN3 or FN1-3 substrates was compared in an ELISA-based assay (Fig. 4 d). Significant direct binding between both $\alpha_v\beta_3$ and $\alpha_5\beta_1$ and FN3 was observed, and both of these interactions were significantly reduced when FN1-3 was used as a substrate (Fig. 4 d). This difference was observed despite a slight disparity in coating efficiency, resulting in the availability of more FN1-3 substrate (Fig. 4 d, inset).

The findings presented clearly demonstrate that the third FN-like repeat of L1 can be recognized by multiple integrins including $\alpha_v\beta_3$, $\alpha_5\beta_1$, and $\alpha_9\beta_1$. However, such interactions are markedly reduced in the presence of FN1. This inhibition is most evident in the case of $\alpha_v\beta_3$ which, when present, appears to have a dominant role in adhesion to FN3, but recognizes FN1-3 poorly.

### *Sequences within the Putative B-C and C-C′ Loop Regions of FN3 Support Integrin Ligation*

Integrin binding motifs in the FN- or Ig-like domains of matrix components or cell adhesion molecules are commonly situated on exposed loops or turns between β-strands. To identify integrin recognition sequences in FN3, we generated a series of peptides corresponding to putative loop regions (Bateman et al., 1996). Two active peptide sequences were identified within the putative B-C and C-C′ loop regions of FN3.

A peptide based on the putative B-C loop sequence RPVDLAQVKGHLR$^{827}$ was found to support significant M21 cell attachment (Fig. 5 a). Overlapping truncation peptides from this sequence established the minimal active sequence to be QVKGHLR$^{827}$. Confirming an integrin-dependent interaction, M21 adhesion to this peptide was blocked using a combination of antibodies to both $\alpha_v\beta_3$ and $\alpha_5\beta_1$ (Fig. 5 b). The adhesion of $\alpha_v(-)$M21-L cells to the QVKGHLR$^{827}$ sequence was blocked by an antibody to $\alpha_5\beta_1$ alone but was unaffected by an mAb to $\alpha_9\beta_1$ (Fig. 5 c). Based on amino acid substitution, both lysine$^{823}$ and the COOH-terminal arginine$^{827}$ residues are essential for adhesion to QVKGHLR$^{827}$ (Fig. 5 d). Substitution of the $NH_2$-terminal glutamine$^{821}$ residue partially reduced adhesion, whereas mutation of histidine$^{825}$ had no effect. Importantly, the corresponding sequence in the mouse L1 homologue (i.e., QVKGHLK) was also able to support adhesion (Fig. 5 d). To confirm direct integrin binding to immobilized QVKGHLR$^{827}$ peptide, binding assays were performed with purified $\alpha_5\beta_1$ and $\alpha_v\beta_3$ heterodimers (Fig. 5, e and f). Significant binding by both $\alpha_v\beta_3$ and $\alpha_5\beta_1$ was observed and, consistent with results obtained in the adhesion assays, mutation of the lysine$^{823}$ residue resulted in the complete loss of binding by both integrins (Fig. 5, e

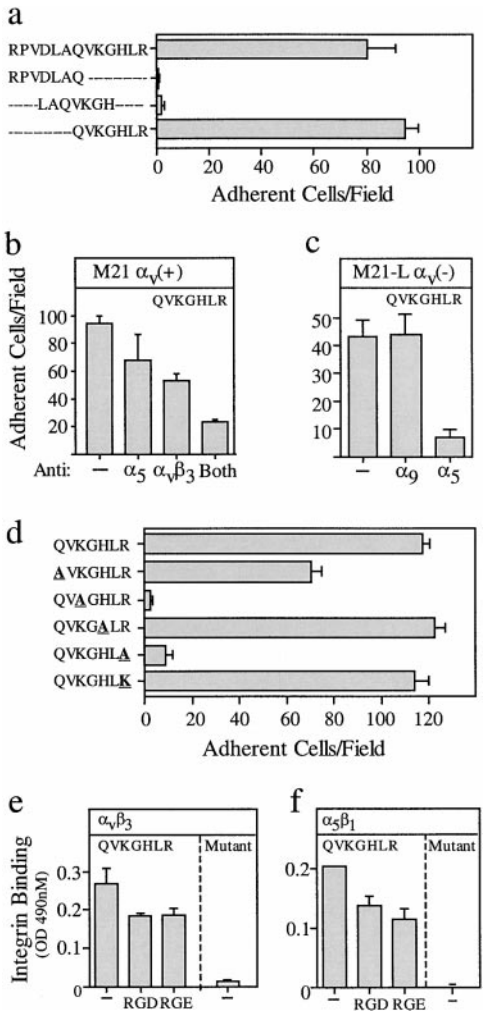


*Figure 5.* A sequence in the putative B-C loop of the FN3 domain supports adhesion via both $\alpha_v\beta_3$ and $\alpha_5\beta_1$. (a) M21 adhesion to an immobilized peptide corresponding to the putative B-C loop of FN3 (RPVDLAQVKGHLR$^{827}$) or overlapping truncation peptides of this sequence. (b) Adhesion of M21 cells to immobilized peptide QVKGHLR$^{827}$ in the presence or absence of antibody to $\alpha_v\beta_3$ (LM609) or $\alpha_5\beta_1$ (P1D6), alone or in combination. (c) Adhesion of $\alpha_v(-)$M21-L cells to immobilized peptide QVKGHLR$^{827}$ in the presence or absence of antibodies to $\alpha_9\beta_1$ (Y9A2) or $\alpha_5\beta_1$ (P1D6). (d) M21 adhesion to peptides resulting from alanine substitutions within the sequence QVKGHLR$^{827}$. (e and f) Direct binding of purified $\alpha_v\beta_3$ (e) or $\alpha_5\beta_1$ (f) integrins to immobilized QVKGHLR$^{827}$ or QV<u>A</u>GHLR$^{827}$ (mutant) peptide as determined by ELISA. Soluble RGD or RGE peptide (50 μg/ml) was added concurrently with the purified integrins. Mutated residues are underlined, and the data shown are the mean of triplicate measurements ± SD.

and f, mutant). Significantly, specific inhibition of integrin binding by the soluble RGD peptide (GRGDSPC) was not detected (Fig. 5, e and f).

A further peptide that was derived from a sequence in the putative C-C′ loop region of FN3 (GSQRKHSKRHIHKDHV[852]) also supported significant cell adhesion (Fig. 6 a). Independent alanine substitution of either of the two dibasic RK[841] and KR[845] sequences within the peptide resulted in a minor loss of cell adhesion, whereas simultaneous mutation of both dibasic sequences abrogated cell adhesion almost completely (Fig. 6 a). Alanine replacement of a downstream KD[850] sequence within the peptide had a negligible effect on cell adhesion, demonstrating the specificity of cell adhesion for the two dibasic sequences. Consistent with these findings, significant cell adhesion was also observed on a 9-mer peptide corresponding to the first half of the entire C-C′ loop peptide (GSQRKHSKR[845]), but not a peptide corresponding to the second half of the C-C′ loop (HIHKDHV[852]; Fig. 6 a). M21 adhesion to the wild-type C-C′ loop peptide GSQRKHSKRHIHKDHV[852] was partially blocked using a combination of antibodies to $\alpha_5\beta_1$ and $\alpha_v\beta_3$ (Fig. 6 b), whereas the adhesion of $\alpha_v(-)$M21-L cells was also partially blocked by inhibition of $\alpha_5\beta_1$, but was not significantly affected by an antibody to $\alpha_9\beta_1$ (Fig. 6 c). It is important to note that a component of M21 cell adhesion to the wild-type GSQRKHSKRHIHKDHV[852] peptide was found to be integrin-independent, with some degree of adhesion evident even in the presence of EDTA (data not shown).

To confirm direct integrin binding to the immobilized GSQRKHSKRHIHKDHV[852] peptide, binding assays were performed with purified $\alpha_5\beta_1$ and $\alpha_v\beta_3$ heterodimers (Fig. 6, d and e). Significant binding to the wild-type peptide by both $\alpha_v\beta_3$ and $\alpha_5\beta_1$ was observed, and independent alanine substitution of either of the two dibasic RK[841] and KR[845] sequences resulted in some loss of binding by both integrins. Concurrent mutation of both dibasic sequences completely abolished binding by both $\alpha_v\beta_3$ and $\alpha_5\beta_1$ (Fig. 6, d and e), which is consistent with results obtained in the adhesion assays. As expected, both integrins bound to the first half of the wild-type peptide exclusively, demonstrating little or no interaction with the second half of the peptide. As with integrin binding to the B-C loop peptide, binding of $\alpha_v\beta_3$ and $\alpha_5\beta_1$ integrins to the C-C′ loop peptide was not specifically inhibited by the soluble RGD peptide (data not shown).

Site-directed mutagenesis of key residues within the putative B-C and C-C′ loop regions of FN3 was performed to confirm that they are required for integrin recognition in the context of the whole domain. Specifically, the sequence QVKGHLR[827] in the putative B-C loop was mutated to QVAGHLR[827], whereas the GSQRKHSKRHIHKDHV[852] sequence constituting the C-C′ loop was mutated to GSQNNHSNNHIHKDHV[852]. Conservative asparagine substitutions were generated within the C-C′ loop to minimize unforeseen effects on domain structure, and both of the dibasic RK[841] and KR[845] sequences were substituted since both were found to contribute to integrin binding (Fig. 6). While the wild-type FN3 domain supported both M21 and $\alpha_v(-)$M21-L adhesion at concentrations as low as 50–75 nM, this adhesion was markedly reduced after substitution of the dibasic sets of lysine and

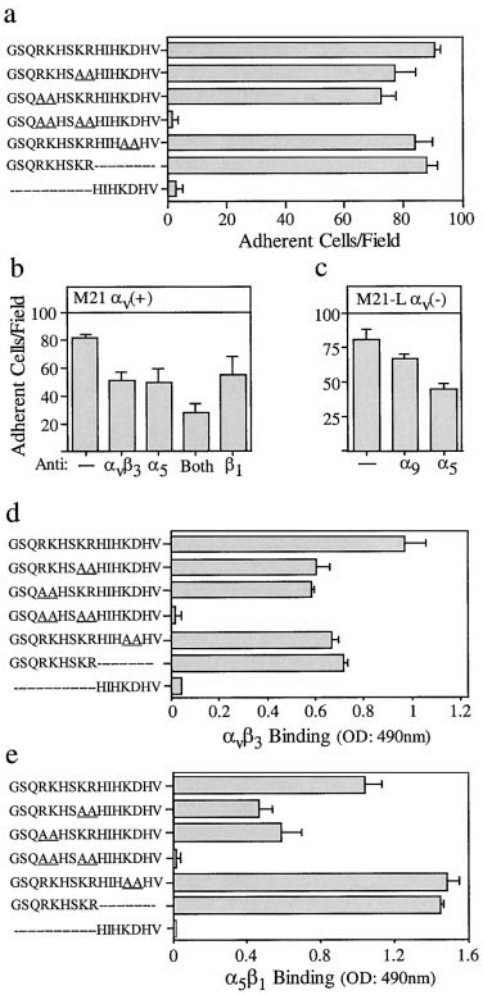


*Figure 6.* A sequence in the putative C-C′ loop of the FN3 domain supports adhesion and is recognized by both $\alpha_v\beta_3$ and $\alpha_5\beta_1$. (a) M21 adhesion to an immobilized peptide derived from a sequence in the putative C-C′ loop of FN3 (GSQRKHSKRHIHKDHV[852]) or peptides resulting from alanine substitution or truncation. (b) Adhesion of M21 cells to immobilized wild-type peptide GSQRKHSKRHIHKDHV[852] in the presence or absence of antibodies to $\alpha_v\beta_3$ (LM609), $\alpha_5\beta_1$ (P1D6), or $\beta_1$ integrins (P4C10), alone or in combination. (c) Adhesion of $\alpha_v(-)$M21-L cells to immobilized wild-type peptide GSQRKHSKRHIHKDHV[852] in the presence or absence of antibodies to $\alpha_9\beta_1$ (Y9A2) or $\alpha_5\beta_1$ (P1D6). (d and e) ELISA determination of the direct binding of purified $\alpha_v\beta_3$ (d) or $\alpha_5\beta_1$ integrins (e) to immobilized wild-type GSQRKHSKRHIHKDHV[852] or mutant peptides derived by alanine substitution or truncation. Mutated residues are underlined, and the data shown are the mean of triplicate measurements ± SD.

arginine residues in the putative C-C′ loop (Fig. 7, a and b). Mutation of the single lysine[823] residue in the putative B-C loop had a relatively small but significant effect on adhesion, which was principally evident at lower coating concentrations (Fig. 7, a and b). To confirm the primary importance of the C-C′ loop sequence, direct binding assays were performed with purified $\alpha_5\beta_1$ and $\alpha_v\beta_3$ integrins. In agreement with the integrin binding results obtained using peptides, ligation of both integrins to the FN3 domain was dose-dependent and saturable, and exhibited significant

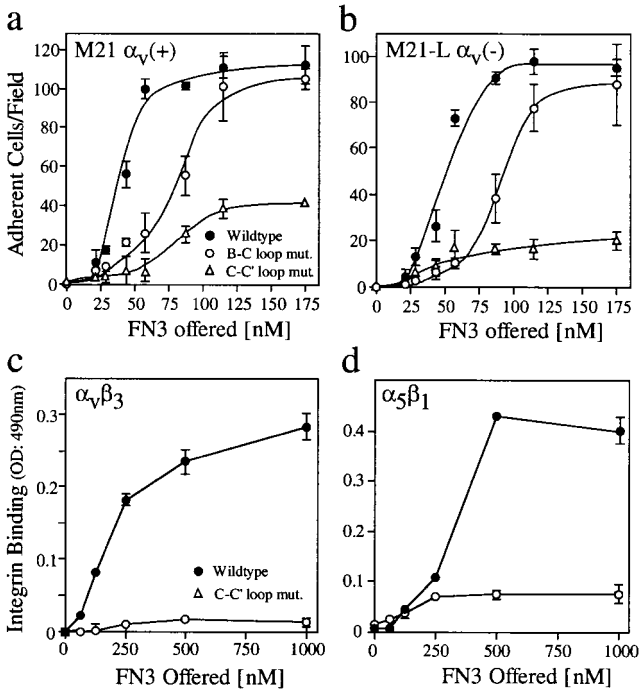


*Figure 7.* Substitution of the dibasic sequences in the putative C-C′ loop of the FN3 domain suppresses adhesion and direct integrin binding. (a and b) Adhesion of M21 (a) or $\alpha_v(-)$M21-L cells (b) to wild-type FN3 domain or mutant FN3 domains containing conservative asparagine substitution of the two dibasic sequences within the C-C′ loop ($RK^{841}$ and $KR^{845}$), or a single $lysine^{823}$ to $alanine^{823}$ substitution within the B-C loop. (c and d) ELISA determination of the direct binding of purified $\alpha_v\beta_3$ (c) or $\alpha_5\beta_1$ integrins (d) to immobilized wild-type FN3 domain or mutant FN3 containing asparagine substitutions within the C-C′ loop. Data shown are the mean of triplicate measurements ± SD.

susceptibility to mutations within the C-C′ loop (Fig. 7, c and d).

Based on our findings, we propose that the FN3 domain of L1 contains two novel integrin binding motifs that account for RGD-independent recognition by $\alpha_5\beta_1$ and $\alpha_v\beta_3$. Substitution studies demonstrate that the dibasic $RK^{841}$ and $KR^{845}$ sequences present in the putative C-C′ loop of FN3 are of primary importance for integrin recognition. A second motif in the putative B-C loop of the FN3 domain ($\underline{Q}V\underline{K}GHL\underline{R}/\underline{K}^{827}$) also contributes to $\alpha_5\beta_1$ and $\alpha_v\beta_3$ binding, albeit to a lesser degree. It is important to note that both $QVKGHLR^{827}$ and $GSQRKHSKRHIHKDHV^{852}$ peptides were ineffective as soluble antagonists in as much as they failed to inhibit adhesion to themselves. Indeed, a paradoxical increase in adhesion was often observed when these peptides were offered during the adhesion assay (data not shown). One explanation for this effect would be that the soluble peptides can self-associate with the immobilized peptide, thereby resulting in multimerized peptide which is then recognized by integrin $\alpha_v\beta_3$ and/or $\alpha_5\beta_1$. While we have obtained clear evidence that $\alpha_9\beta_1$ can support adhesion to FN3, we failed to identify the binding motif. It may prove that recognition by this integrin is subject to conformational constraints that are violated by the use of linear peptides.

### *Integrins Recognize Multimerized FN3 and Homoaggregation of This Domain Is Regulated by the Dibasic Sequences in the Putative C-C′ Loop and by the Presence of FN1*

Purified FN3 and FN2-3 fusion proteins (GST or His) were both observed to precipitate at high protein concentrations, suggesting a propensity for homoaggregation. In contrast, such precipitation was not observed with either Ig6-FN1-3 or FN1-3 fusion proteins. These observations, coupled with the prior observation that the presence of FN1 is inhibitory to cell adhesion on FN3, raised the possibility that integrins preferentially recognize the FN3 domain as a homomultimer and that inhibition of integrin recognition by FN1 is related to the ability of this domain to inhibit such multimerization. It was also observed that precipitation of the FN3 domain was markedly reduced after substitution of the dibasic $RK^{841}$ and $KR^{845}$ sequences present in the putative C-C′ loop sequence of FN3. This raised the further possibility that the peptide sequence $GSQRKHSKRHIHKDHV^{852}$, which is of primary importance for integrin recognition, is also important for FN3 homomultimerization. Indeed, a propensity for self-association by the $GSQRKHSKRHIHKDHV^{852}$ peptide could explain the paradoxical finding that this peptide can function as a soluble agonist in adhesion assays. Confirmation of this hypothesis would require that several stipulations be fulfilled: (1) FN3 is multimerized at the time of integrin recognition; (2) the presence of FN1 limits FN3-mediated multimerization; and (3) the GSQRKHSKRHIHKDHV$^{852}$ peptide self-associates and mutation of the C-C′ loop sequence, which results in a loss of integrin recognition, also prevents multimerization.

As a first step, we looked for evidence of FN3 multimerization by both column chromatography and SDS-PAGE. To avoid potential complexities associated with the presence of GST as a fusion partner, these studies were performed with an FN3-His construct. After gel filtration on a Sephracryl S-200 column, the FN3 domain was observed to elute as a series of high molecular mass complexes (Fig. 8 a, top). Based on size relative to molecular mass standards, the smallest complexes were trimers (3×) and hexamers (6×), with relatively little monomer (1×) evident. The relative proportion of monomer present in different preparations varied with some preparations having little or no evidence of any monomer whatsoever. It should be noted that any precipitate present in the FN3 preparations was removed by centrifugation before fractionation by column chromatography. In support of these findings with the FN3-His protein, separation of the FN3-GST preparation also revealed the presence of trimeric and higher order complexes (data not shown).

Upon SDS-PAGE resolution under nondenaturing conditions (i.e., without boiling), most of the FN3–His complexes were resolved into the monomer (16 kD, 1×; Fig. 8 b, lane 1). However, even in the presence of SDS, a significant amount of trimeric FN3 (48 kD, 3×) was detected. Depending upon the amount of material loaded, small amounts of hexameric FN3 (96 kD, 6×) and sometimes even higher order species could also be detected (Fig. 8 b, lane 1). Taken together, these data demonstrate that, under native conditions, the FN3 domain self-associates to

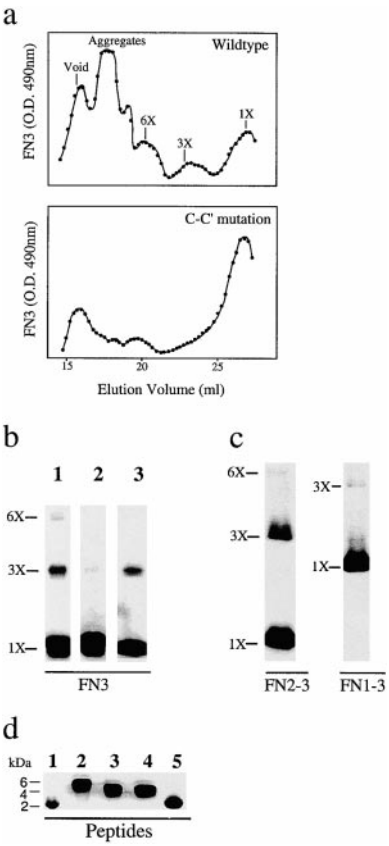


*Figure 8.* Homomultimerization of the FN3 domain is mediated by dibasic sequences in the putative C-C′ loop and regulated by the presence of FN1. (a) Sephacryl S-200 gel filtration elution profiles of wild-type FN3 domain (top) or mutant FN3 containing conservative asparagine substitution of the two dibasic sequences (RK[841] and KR[845]) within the C-C′ loop (bottom). Elution points of monomer (1×), trimer (3×), and hexamer (6×) in relation to molecular mass standards are denoted. (b) SDS-PAGE analysis of wild-type FN3 (lane 1), FN3 in which the two dibasic pairs within the C-C′ loop are replaced with asparagines (lane 2), or FN3 in which lysine[823] within the B-C loop is replaced with alanine (lane 3). Separated proteins were detected by immunoblotting with the anti–L1 ECD pAb. (c) SDS-PAGE and immunoblot comparison of FN3 in conjunction with adjacent FN-like domains (FN2-3 or FN1-3). The relative migration of monomeric (1×), trimeric (3×), and hexameric species (6×) are indicated. (d) SDS-PAGE comparison of wild-type GSQRKHSKRHIHKDHV[852] peptide (lane 2), with single dibasic alanine mutant peptides (GSQAAHSKRHIHKDHV[852], lane 3; GSQRKHSAAHIHKDHV[852], lane 4) and the double dibasic alanine mutant peptide (GSQAAHSAAHIHKDHV[852], lane 5). A peptide derived from the Ig6 domain of L1 (PSITWRGDGRDLQEL[544]) is shown for comparison (lane 1). The relative migration of the peptides in relation to molecular mass standards is shown at the left.

form large multimeric complexes and that the most stable multimeric configuration appears to be a trimer (SDS-PAGE), which can further self-associate to form higher order complexes (gel filtration).

Importantly, substitution of the dibasic RK[841] and KR[845] sequences present in the putative C-C′ loop sequence of FN3, which effectively abrogated integrin binding, was also found to limit FN3 multimerization. This is demonstrated by the large amount of monomeric FN3 evident on fractionation (Fig. 8 a, bottom) and by an almost complete absence of trimeric FN3 (3×) evident on SDS-PAGE (Fig. 8 b, lane 2). The small amount of complexed FN3 remaining despite mutation of the dibasic sequences likely reflects the conservative substitution of the arginine and lysine residues with asparagines. In contrast, alanine mutation of the lysine[823] residue in the putative B-C loop, which only marginally effected adhesion, did not obviously effect the multimerization of FN3 (Fig. 8 b, lane 3). This lack of effect on domain multimerization was also observed upon fractionation of the lysine[823] mutant by gel filtration (data not shown). Together, these data suggest that integrin binding to FN3 primarily involves recognition of multimers.

Confirming the hypothesis proposed above, a comparison of complex formation by FN1-3 versus FN3 demonstrates that the presence of FN1 does indeed limit multimerization mediated by the FN3 domain. Thus, the proportion of trimeric FN1-3 (140 kD, 3×) evident on SDS-PAGE was found to be markedly lower than that observed with both FN3 (Fig. 8 b, lane 1) and FN2-3 (Fig. 8 c). That the FN2-3 construct forms complexes as efficiently as FN3 is consistent with the ability of this two-domain construct to support adhesion at levels equivalent to FN3 alone (Fig. 3 a). The observation that FN1-3 is still capable of limited multimerization may explain why FN1-3 can still be recognized by integrins at high coating concentrations.

A final requirement of the hypothesis proposed above is that the GSQRKHSKRHIHKDHV[852] peptide derived from the C-C′ loop of FN3 can self-associate and, as a result, support integrin recognition as a peptide complex. This would support the concept that the C-C′ loop of FN3 promotes both multimerization and integrin binding. On SDS-PAGE the 16-mer GSQRKHSKRHIHKDHV[852] peptide, which has a predicted molecular mass of 2 kD, was found to migrate as a primary species of ~6 kD, indicative of an SDS-stable tripeptide complex (Fig. 8 d, lane 2). A 15-mer peptide of 1.95 kD derived from the Ig6 domain of L1 (PSITWRGDGRDLQEL[544]) is shown for comparison (Fig. 8 d, lane 1). Interestingly, separate alanine substitution of either of the two dibasic RK[841] or KR[845] sequences in the GSQRKHSKRHIHKDHV[852] peptide resulted in a reduction in molecular mass, which is consistent with the formation of di- rather than tripeptide complexes (Fig. 8 d, lanes 3 and 4). Finally, simultaneous alanine replacement of both sets of dibasic residues resulted in a peptide that resolved as a monomeric species (Fig. 8 d, lane 5). Importantly, these same alanine substitutions also abrogated cell adhesion and integrin binding (Fig. 6). Taken together, these data indicate that optimal integrin binding to the GSQRKHSKRHIHKDHV[852] peptide under native conditions involves recognition of tripeptide or higher order peptide complexes and confirms a role for the dibasic RK[841] and KR[845] sequences in domain and peptide multimerization.

### *Plasmin Regulates FN3 Multimerization and Integrin Binding*

Human L1, as well as related molecules in the mouse, rat (NILE), and chick (Ng-CAM and Nr-CAM) have been

shown to be sensitive to posttranslational cleavage within the FN3 domain (Faissner et al., 1985; Sadoul et al., 1988; Nybroe et al., 1990; Burgoon et al., 1995). Importantly, this cleavage has been shown to involve the same dibasic sequences that we have identified as important for integrin binding and multimerization. Thus, trypsin has been shown to cleave after the second dibasic sequence (GSQRKHSKR$^{\downarrow}$HIHKDHV$^{852}$; Faissner et al., 1985; Sadoul et al., 1988), whereas we have recently demonstrated that plasmin cleaves both dibasic sequences (GSQ-RK$^{\downarrow}$HSK$^{\downarrow}$RHIHKDHV$^{852}$; Nayeem et al., 1999). Based on this information, we questioned whether posttranslational cleavage of the FN3 domain represents a mechanism for regulating both multimerization and integrin binding.

Treatment of FN3–His complexes with plasmin resulted in a dose-dependent dissolution of the trimeric FN3 complexes evident on SDS-PAGE (Fig. 9 a). A loss of trimeric FN3 complexes was evident at plasmin concentrations as low as 0.01 U/ml. Consistent with this finding, treatment of immobilized FN3 substrate with plasmin at a concentration of 0.01 U/ml also resulted in a >60% inhibition of adhesion by both M21 and $\alpha_v(-)$M21-L cells (Fig. 9 b, right). At the same concentration, plasmin had no effect on the RGD-dependent adhesion of M21 cells to the Ig6 domain of L1 (Fig. 9 b, left). Interestingly, plasmin treatment of the L1 ectodomain also resulted in a marked inhibition of adhesion by $\alpha_v(-)$M21-L cells, but only marginally decreased adhesion by M21 cells (Fig. 9 b, middle). This result is consistent with the finding that $\alpha_v(-)$M21-L adhesion to the L1 ectodomain is highly dependent on interactions with the FN3 domain, while M21 cells can still adhere via interaction with the RGD motif in the Ig6 domain. Together, these data support the concept that serine protease–mediated cleavage within the FN3 domain is a potentially important mechanism for regulating its functional activity.

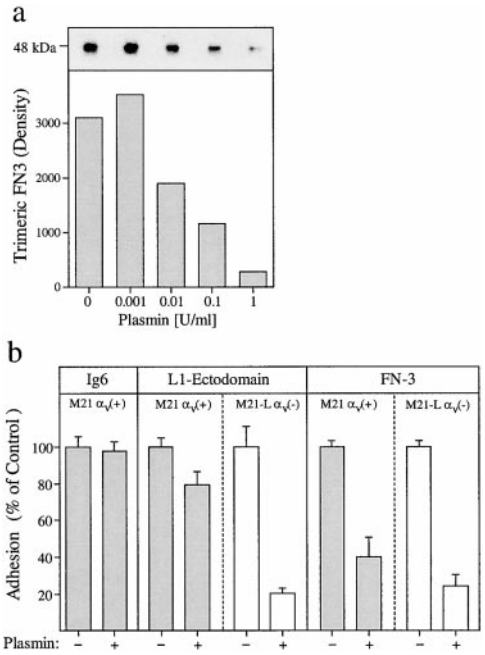


*Figure 9.* Plasmin regulates FN3 multimerization and integrin binding. (a) SDS-PAGE and immunoblotting analysis of complexed wild-type FN3 treated with plasmin. FN3 in solution was treated for 90 min with plasmin before SDS-PAGE and immunoblotting with the anti–L1-ECD pAb. The FN3 trimer band (48 kD) was analyzed by scanning densitometry and graphed in arbitrary density units. (b) Adhesion of M21 or $\alpha_v(-)$M21-L cells to Ig6, FN3, or L1 ectodomain treated with plasmin. Immobilized proteins were treated with or without 0.01 U/ml plasmin for 90 min, washed, and blocked before the addition of cells. Data shown are the mean of triplicate measurements ± SD.

### *A Paradigm for L1–Integrin Interactions*

Based on our findings, it is evident that FN1 limits homomultimerization via the FN3 domain. One possible explanation for this would be steric hindrance in which the FN1 and FN3 domains are folded back upon one another in a closed globular conformation. Homomultimerization via the FN3 domain and concomitant integrin recruitment may only occur after a change in conformation that promotes a more extended open configuration. Homophilic L1–L1 ligation via the Ig-like domains and/or integrin interaction with the RGD motif in Ig6 may be mechanisms for inducing such a change in conformation. A schematic representation of such a model is shown in Fig. 10 a.

Certain predictions can be made based on the model proposed. First, it should be possible to show that, as a result of folding between FN1 and FN3, accessibility to certain domain regions will be limited. In this regard, an mAb specific for an epitope in the Ig6 domain of L1 (mAb LP1B9) was able to recognize Ig6-FN1 and Ig6-FN1-2, but was very limited in its ability to recognize Ig6-FN1-3 (Fig. 10 b). This result is hard to reconcile if Ig6-FN1-3 simply forms a linear structure, but can be explained readily if there is a folding event that juxtaposes FN3 with FN1 and Ig6.

A further prediction of the model presented is that inhibition of upstream L1 ligation (e.g., homophilic L1–L1 ligation) will also inhibit integrin-dependent adhesion via FN3 because the FN-like repeats will remain in a closed conformation. In this regard, we observed that integrin-dependent adhesion of $\alpha_v(-)$M21-L cells to the L1 ectodomain could be significantly reduced by an antibody (5G3) that blocks homophilic L1–L1 ligation by binding to an $NH_2$-terminal Ig-like domain (Montgomery et al., 1996; Nayeem et al., 1999; Fig. 10 c, left). It is unlikely that this antibody is inhibiting $\alpha_v(-)$M21-L adhesion by directly blocking integrin recognition of the FN3 domain since it recognizes a distal epitope and fails to prevent integrin binding to the Ig6 domain, which is located closer to the antibody binding site. However, since $\alpha_v(-)$M21-L cells express high levels of L1, a homophilic interaction with the immobilized L1 could induce the conformation change required for binding of these cells to FN3. The 5G3 antibody was markedly less effective at preventing M21 cell adhesion to the L1 ectodomain (Fig. 10 c, right), presumably because these cells are still able to recognize the RGD motif in the Ig6 domain via $\alpha_v\beta_3$. It is interesting to note that the 5G3 antibody also had some minimal inhibitory activity when the FN3 domain alone was offered as a substrate (Fig. 10 c). This inhibition may indicate a limited but direct interaction between cellular L1 and the immobilized FN3

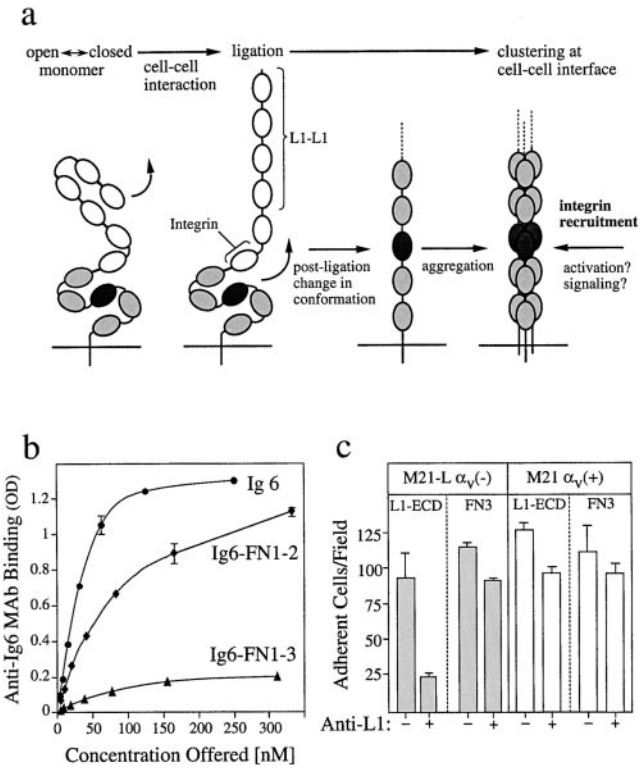


*Figure 10.* L1 conformation and L1–L1 homophilic interaction may regulate integrin recruitment via the FN3 domain. (a) A potential model for the interaction between integrins and the FN3 domain of L1. The Ig- and FN-like domains of L1 are assumed to form a closed globular conformation according to the findings of Su et al. (1998) and Drescher et al. (1996). Distal ligation events involving the Ig-like domains of L1 (L1–L1 or L1–integrin) are postulated to cause a conformational change, resulting in a permissive open conformation that can support L1 clustering via FN3 and subsequent integrin recruitment. Potential implications of this multimerization and integrin recruitment include L1-integrin–dependent signal transduction. (b) Anti-Ig6–specific mAb (LP1B9) recognition of its epitope in the Ig6 domain alone, or Ig6 with adjacent FN-like domains (Ig6-FN1-2 and Ig6-FN1-3) as determined by ELISA. Immobilized proteins were incubated with the anti–L1-Ig6 mAb LP1B9, washed, and were detected colorimetrically with HRP-conjugated secondary antibody and OPD. (c) Adhesion of M21 or $\alpha_v(-)$M21-L cells to the L1 ectodomain (L1-ECD) or FN3 after pretreatment of cells with the function-blocking anti-L1 mAb 5G3. Data shown are the mean of triplicate measurements ± SD.

domain. In this regard, it has been shown that FN constructs containing the FN3 domain can interact with other Ig-like domains present in the L1 ectodomain (Holm et al., 1995).

Based on the premise that distal L1 ligation events are required to promote FN3 multimerization and integrin recruitment, it is also to be expected that L1 and integrins will only colocalize at the cell–cell interface, where such distal ligation events are expected to occur. Double immunofluorescence was performed to test this prediction. The $\alpha_9\beta_1$ integrin was selected for analysis since previous studies with the $\alpha_v(-)$M21-L cells demonstrated that this integrin is primarily involved in adhesion to the FN3 domain rather than the RGD motif in Ig6. Aggregates of $\alpha_v(-)$M21-L cells were analyzed after simultaneous staining for $\alpha_9\beta_1$ and L1. Both L1 and $\alpha_9\beta_1$ were observed to be recruited to sites of cell–cell contact (Fig. 11, a and b) and significant colocalization is evident at these sites (Fig. 11, c and d). However, it is also important to note that these ligands do not appear to colocalize unless recruited to the cell–cell interface as demonstrated by confocal microscopic analysis (Fig. 11 d). Since the juxtaposition of two cell membranes could give the illusion of colocalization, it was further determined whether such colocalization is still evident on single cells obtained after the gentle disruption of stained cell aggregates. The disruption of cell aggregates was performed with simultaneous fixation. Using this approach, we observed significant modulation of both L1 and $\alpha_9\beta_1$ on some of the single cells obtained (Fig. 11, e and f). Based on the absence of such obvious modulation in the absence of prior aggregation, it is likely that areas of modulation are a result of prior cell–cell contact. Importantly, even under these conditions, we still observed significant colocalization of L1 and $\alpha_9\beta_1$ (Fig. 11 g). Significant colocalization was not observed on those single cells that failed to display evidence of modulation (Fig. 11 g, asterisk). Adopting the same experimental approach, but with all steps performed at 37°C in the absence of sodium azide, we observed further marked modulation of L1 and $\alpha_9\beta_1$ expression (Fig. 11, h and i), and again significant colocalization was observed (Fig. 11 j). Colocalization between $\alpha_9\beta_1$ and L1 on individual cells that were separated from cell aggregates supports the concept of a cis-interaction between these two ligands.

As a further test of a direct association between $\alpha_9\beta_1$ and L1, coimmunoprecipitation studies were performed using the anti-$\alpha_9\beta_1$ mAb Y9A2. Cell lysates were made from $\alpha_v(-)$M21-L cells maintained as aggregates or as subconfluent monolayers. These lysates were treated with mAb Y9A2 and Western blot analysis was performed to detect the presence of coprecipitated L1. Consistent with an interaction at sites of cell–cell contact, L1 was readily detected in Y9A2 immunoprecipitates derived from lysates of aggregated $\alpha_v(-)$M21-L cells (Fig. 11 k, Agg.). In contrast, only minimal reactivity was evident in the lysate derived from monolayer cultures (Fig. 11 k, Mono.). As further confirmation of L1–integrin association, reverse immunoprecipitation was performed using an anti-L1 polyclonal antibody (anti-5G3 Ag-pAb). In these studies, Western blot analysis was performed to detect the presence of coprecipitated $\beta_1$, $\alpha_5$, $\beta_3$, and $\beta_5$ integrin subunits. Providing further evidence for a possible association between L1 and $\alpha_9\beta_1$, Western blot analysis confirmed the presence of the $\beta_1$ integrin subunit in immunoprecipitates derived from aggregated $\alpha_v(-)$M21-L cells (Fig. 11 l). Because of a lack of antibodies suitable for the detection of the $\alpha_9$ subunit by Western blotting, we cannot definitively claim that the presence of the $\beta_1$ integrin subunit is due to the coprecipitation of $\alpha_9\beta_1$. However, given that $\alpha_9\beta_1$ both colocalizes with and coprecipitates L1, it is likely that at least a component of the $\beta_1$ present is due to its association with $\alpha_9$. Consistent with reports that have indicated an association between L1 and $\alpha_5\beta_1$ and $\alpha_v\beta_3$, both $\beta_3$ and $\alpha_5$ integrin subunits were also identified in immunoprecipitates of aggregated M21 or M21-L cells (Fig. 11 l). In contrast, despite the presence of significant amounts of $\alpha_v\beta_5$ in M21

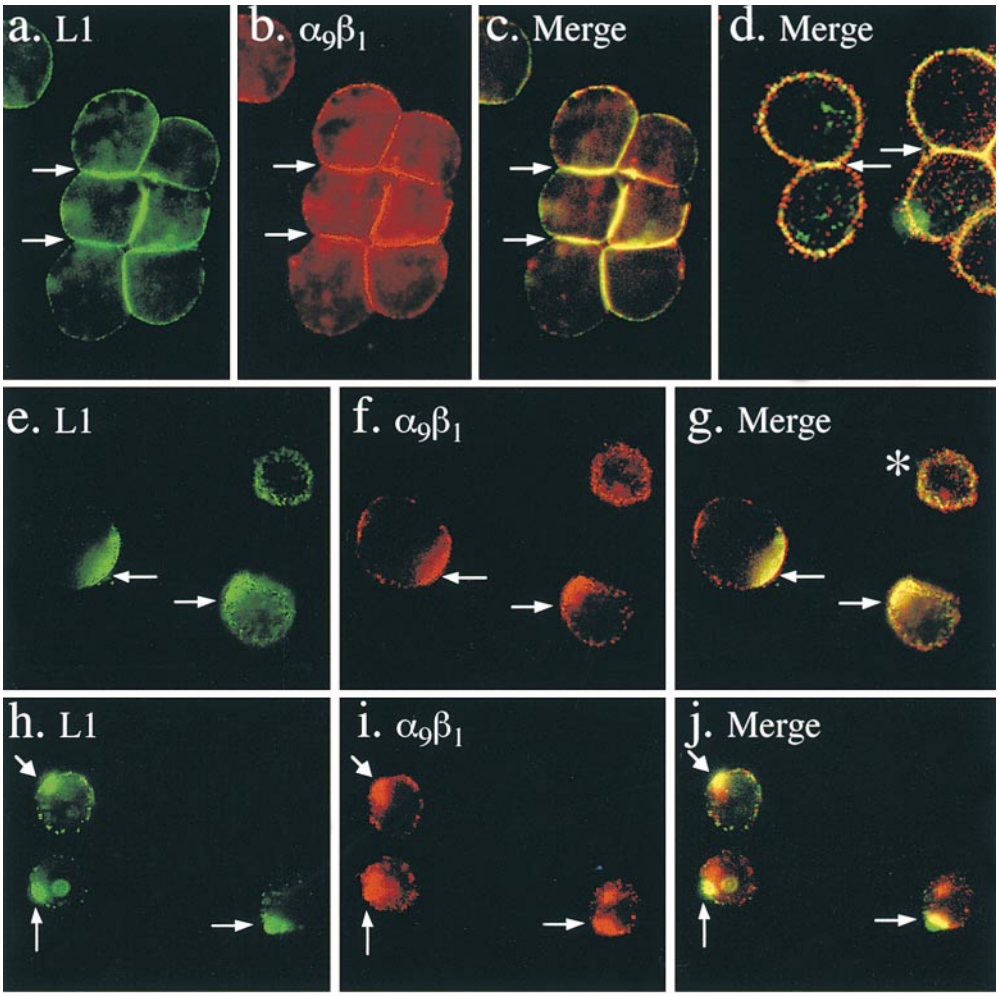


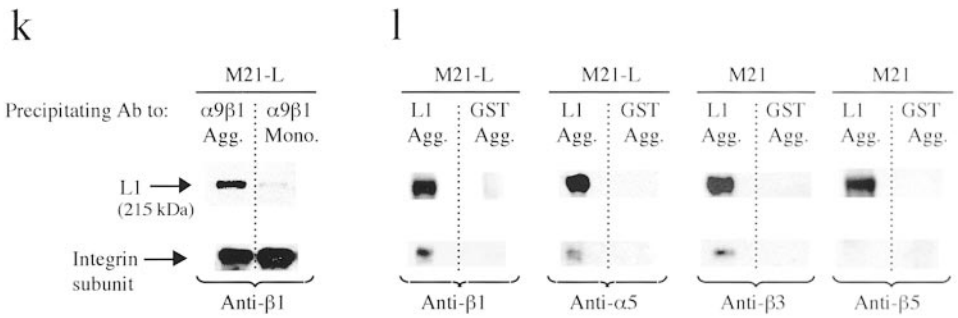


*Figure 11.* Colocalization and coimmunoprecipitation of L1 and integrins after cell–cell interaction. (a–c) Staining of M21-L cell cluster with anti–L1-ECD pAb and the anti-$\alpha_9\beta_1$ mAb Y9A2. L1 staining is shown in green (a, FITC), $\alpha_9\beta_1$ staining in red (b, Texas red), and overlapping fluorescence or colocalization is evidenced as yellow (c, Merge). Arrows denote areas of colocalization at points of cell–cell contact. Images were obtained using a 40× objective and a Nikon Eclipse E800 fluorescent microscope. (d) Merged image of L1 (green) and $\alpha_9\beta_1$ (red) staining of M21-L cell clusters obtained using an MRC 1024 confocal microscope. Note that colocalization is primarily limited to cell–cell interfaces (arrows). (e–g) Disruption of stained M21-L cell clusters with simultaneous fixation results in some single cells with areas of modulated L1 and $\alpha_9\beta_1$ expression (e and f). Note that there is still evidence of significant colocalization between L1 and $\alpha_9\beta_1$(g). No significant localization was observed in another cell that failed to show evidence of L1 or $\alpha_9\beta_1$ modulation (g, asterisk). (h–j) M21-L cell clusters were stained at 37°C and in the absence of azide. After disruption of cell aggregates, some single cells showed evidence of significant L1 and $\alpha_9\beta_1$ modulation (h and i). Significant areas of colocalization were observed (j). (k) Coimmunoprecipitation of L1 with an anti-$\alpha_9\beta_1$ mAb. Lysates were obtained from aggregated $\alpha_v(-)$M21-L cells (Agg.) or their adherent subconfluent counterparts (Mono.). Precipitated proteins were immunoblotted to detect coprecipitated L1 or the immunoprecipitated $\beta_1$ subunit of $\alpha_9\beta_1$. (l) Reverse immunoprecipitation was performed using an anti-L1 pAb and lysates of aggregated M21-L or M21 cells. A polyclonal antibody to GST was used as a control. Immunoprecipitated material was immunoblotted using antiintegrin antibodies as described in Materials and Methods. Membranes were reprobed with anti-L1 mAb 5G3 to confirm precipitation of L1. Integrin subunits identified have molecular masses consistent with that reported in the literature.

cell lysates, no significant coprecipitation of the $\beta_5$ subunit was detected (Fig. 11 l). Importantly, none of the integrin subunits were detected after immunoprecipitation using a control antibody to GST (Fig. 11 l).

Based on the observation that L1–integrin colocalization is primarily restricted to sites of cell–cell contact, it is to be expected that only a small fraction of the available integrin pool will be directly associated with L1. In our system, despite attempts to maximize aggregation, we still observed that many cells remained single and, even in aggregates, we often observed variable recruitment into cell–cell contact sites. It also needs to be recognized that some integrins are sequestered in large intracellular pools. In the case of the $\beta_1$ integrin subunit, the amount specifically co-

precipitated with L1 appears to be <1% of the total available cellular $\beta_1$. However, since the L1-reactive $\beta_1$ integrins (i.e., $\alpha_5\beta_1$ and $\alpha_9\beta_1$) constitute only a small fraction of the total $\beta_1$ integrin expression by M21-L cells (<10%) this is not unexpected. Consistent with this, we estimate that significantly more of the available $\alpha_5\beta_1$ integrin pool coprecipitated with L1 (~5%). However, such estimates may be underestimates since it is not clear how stable L1–integrin complexes are under the detergent conditions used during the immunoprecipitation.

## *Discussion*

In this study, we have shown that integrin binding to intact L1 cannot be solely attributed to the RGD motif present in the sixth Ig-like domain, but rather involves additional recognition of sequences in the third FN-like domain (FN3). As such, we describe two novel integrin-binding motifs located within the putative B-C and C-C′ loops of the FN3 domain (QVKGHLR$^{827}$ and GSQRKHSKR$^{845}$). Site-directed mutagenesis of key residues within these motifs confirmed the primary importance of the sequence GSQRKHSKR$^{845}$ for both cell adhesion and direct integrin binding to the FN3 domain. Remarkably, the same dibasic sequences responsible for supporting integrin binding to this motif (RK$^{841}$ and KR$^{845}$) are also shown to promote the multimerization of the FN3 domain. In this regard, multimerization of the GSQRKHSKR$^{845}$ sequence precedes, and may be required for, interaction with both $\alpha_v\beta_3$ and $\alpha_5\beta_1$ integrins. Importantly, both homomultimerization of, and integrin binding to FN3 is shown to be regulated both by conformational constraints imposed by other FN-like domains (FN1) and by plasmin-mediated cleavage within the sequence RK$^{\downarrow}$HSK$^{\downarrow}$RH$^{846}$. Based on our findings, we propose that L1 may have an expanded role in the regulation of integrin function, especially at the cell–cell interface, where bridging events appear to allow L1–integrin ($\alpha_9\beta_1$) colocalization.

The large multidomain organization of L1 has permitted the evolution of domains and domain regions with distinct functional attributes. A recent model based on the crystal structure of hemolin suggests that an antiparallel alignment involving the first four Ig-like domains of L1 is responsible for homophilic L1–L1 binding (Su et al., 1998). Importantly, the same Ig-like domains involved in homophilic binding may also adopt a tertiary horseshoe configuration because of acute folding and strong interdomain pairing (Su et al., 1998), suggesting that homophilic L1–L1 binding at the cell surface may be regulated by an equilibrium between open/accessible (extended) and closed/inaccessible (globular or horseshoe shaped) conformations within the distal Ig domains.

In this study, we propose that the functional activity of the FN-like domains of L1 may also be regulated by open (extended) and closed (globular) conformations. In this regard, a recent structural analysis of L1 by rotary shadowing and transmission electron microscopy confirmed that the FN-like repeats do indeed form a tight globular structure (Drescher et al., 1996). In addition, an antibody directed towards an epitope located between domains FN2 and FN3 mimics the effects of homophilic L1–L1 binding, promoting neurite outgrowth and signal transduction (Appel et al., 1995). Based on their findings, the authors suggest that conformational changes resulting from L1 ligation could funnel to this region of L1, a region that may be conformationally labile and the ultimate site for the induction of signaling events. Together, these findings are consistent with the paradigm that the FN-like repeats assume a closed globular conformation and that extrinsic ligation, by an antibody or by L1 itself, has important functional consequences by virtue of exposing a region that is essential for receptor multimerization, integrin recruitment, and consequent cell signaling.

While we suggest that homophilic ligation can alter the conformation of the FN-like repeats, thereby exposing the FN3 domain and promoting integrin recruitment, other heterophilic interactions may also have a role. In this regard, it is of particular interest that TAG-1/axonin-1, a neuron-specific CAM, has been shown to promote neurite extension via a mechanism that requires both an L1-like molecule and β1 integrins (Felsenfeld et al., 1994). The authors suggest a mechanism involving a direct interaction between TAG-1 and L1, leading to a concomitant cis-interaction between L1 and $\beta_1$ integrin. The result of these interactions is signaling via both types of receptors, thereby culminating in neurite extension. A further possibility is that a direct trans-interaction between integrins and the RGD motif in the Ig6 domain of L1 is sufficient to funnel a conformational change to the adjacent FN-like repeats. This type of interaction would facilitate L1 multimerization and further integrin recruitment, even when the interacting cell type fails to express neuron-associated CAMs.

The concept that the FN3 domain is involved in self-association is supported by earlier work, which showed that beads coated with FN-like domains 3–5 of L1 had a strong tendency to self-associate (Holm et al., 1995). Consistent with a central role for the FN3 domain in this process, little or no aggregation was observed with beads coated with FN-like domains 1 and 2 or 4 and 5. Furthermore, and in accordance with our finding that the FN1 domain limits multimerization through FN3, the authors also observed that beads coated with FN-like domains 1–5 showed little tendency towards self-association. Our finding that the FN3 domain can support cell adhesion is also supported in the literature. Thus, Appel et al. (1993) demonstrated strong neural cell adhesion to an L1 fragment consisting of FN-like domains 3–5. In agreement with our findings, little adhesion was observed on FN-like domains 1 and 2. Again supporting a negative regulatory function for the FN1 domain in this process, the adhesion observed on FN-like domains 1–5 was markedly reduced in comparison to that evident on FN-like domains 3–5. While the authors suggested that the neuronal adhesion observed was primarily due to homophilic ligation between cellular L1 and the L1 fragments, they also proposed a role for an unidentified heterophilic ligand. Based on the findings presented in this manuscript, neuronal integrins would be likely candidates for this role.

Based on our findings, we propose that the FN3 domain is of essential importance for the biological activity of L1. As a consequence, it is expected that the activity of this domain will be tightly regulated. While we propose that conformational constraints are a primary mechanism for

regulating the activity of FN3, we also detail a second mechanism based on proteolytic cleavage. An important and unifying property of L1-like proteins is a susceptibility to posttranslational cleavage, thus, human and mouse L1, as well as related molecules in the rat and chick, are sensitive to cleavage within the FN3 domain, yielding fragments that have been detected in neural tissue in vivo (Rathjen and Schachner, 1984; Faissner et al., 1985; Sadoul et al., 1988; Wolff et al., 1988; Nybroe et al., 1990; Burgoon et al., 1995). Cleavage within the FN3 domain is due to the presence of a highly conserved serine protease–sensitive region that incorporates dibasic arginine/lysine sequences (Faissner et al., 1985; Sadoul et al., 1988). Significantly, we have now shown that this same sequence of basic amino acids is important for FN3 multimerization and integrin binding. Furthermore, we show that low concentrations of plasmin will disrupt such interactions, even in the case of pre-formed complexes, based upon the ability of plasmin to cleave within the sequence $RK^{\downarrow}HSK^{\downarrow}RH$ (Nayeem et al., 1999). This suggests that plasmin-mediated proteolysis of homomultimerized FN3 domains may provide an important mechanism for regulating initiation and/or inactivation of L1–integrin interactions. Potential regulation of L1 function by plasmin is of particular interest, given the extensive overlap of neurological functions that involve both plasmin and L1 including neurite extension (Lagenaur and Lemmon, 1987; Seeds et al., 1997), granule cell migration (Krystosek and Seeds, 1981; Moos et al., 1988), nerve regeneration (Salles et al., 1990; Jung et al., 1997), and long-term potentiation in the hippocampus (Luthl et al., 1994; Mizutani et al., 1996).

The extent to which the FN3 domain promotes either cis- or trans-integrin interactions remains to be resolved. Multimerization of L1 in the plane of the cell membrane via a domain (i.e., FN3) that is in close proximity to the membrane may favor the recruitment of integrins in a cis-type of interaction. The demonstration of colocalization between $\alpha_9\beta_1$ and L1 on individual cells separated from cell aggregates supports the concept of a cis-interaction. In this regard, cis-interactions between integrins and other receptors, including members of the IgSF, are well documented and are believed to be an important mechanism for both regulating the activational status of the integrin, and for the formation of signaling complexes at the cell–cell or cell–substrate interface (Porter and Hogg, 1998). While conformational constraints are proposed to regulate integrin access to the FN3 domain, such constraints are less likely to limit integrin recognition of the RGD motif in the Ig6 domain of L1. Thus, Drescher et al. (1996) conclude that the RGD motif in human L1 is available for intermolecular interactions based both on the high surface hydrophobicity of the Ig6 domain and the position of the motif within a loop structure. Based on this, it is conceivable that RGD-dependent integrins can recognize L1 (Ig6) in its resting conformation via a trans-interaction at the cell–cell interface. Whether such an interaction is sufficient to initiate a conformational change in L1 and further integrin recruitment via a cis-non-RGD–dependent mechanism remains to be determined. It is also unclear whether recognition of FN3 by integrins involves the typical ligand-binding pocket or is the result of an interaction with alternative sites on either or both of the integrin subunits. Specificity for $\alpha_5\beta_1$ and $\alpha_9\beta_1$ to the apparent exclusion of other $\beta_1$ integrins does, however, suggest the involvement of the $\alpha$-subunit.

Changes in L1 conformation and concomitant L1 clustering may also be important for the recruitment of other heterophilic ligands reported to undergo cis-interactions with L1. Candidate ligands include the following: CD9 (Schmidt et al., 1996), NCAM (Feizi, 1994), CD24 (Kadmon et al., 1995), axonin-1/TAG-1 (Kunz et al., 1998), and the FGF receptor (FGFr; Viollet and Doherty, 1997). It is conceivable that L1 clustering results in the recruitment of a variety of signaling elements (e.g., CD9, CD24, and FGFr) culminating in the formation of large signaling complexes at the cell–cell interface. In this regard, it has been suggested that trans-homophilic L1–L1 ligation leads to L1 clustering and the recruitment of FGFr (Viollet and Doherty, 1997). Downstream signaling events resulting from the activation of the FGF tyrosine kinase receptor have now been shown to be responsible for L1-mediated neurite extension (Viollet and Doherty, 1997). The potential recruitment of CD9 is also of particular interest since this tetraspan signaling molecule is also known to associate with certain integrins (Berditchevski and Odintsova, 1999) and could, therefore, serve to stabilize cis-complexes formed between integrins and L1. Given the pivotal importance of the third FN-like repeat of L1, it may prove significant that this domain also has been implicated in the cis-interaction between the chick L1 orthologue NgCAM and axonin-1/TAG-1 (Kunz et al., 1998). While we speculate that changes in L1 conformation and concomitant L1 clustering could result in the recruitment of a variety of signaling molecules, we do not exclude the possibility that certain cis-interacting ligands may compete with or inhibit integrin recruitment or that some heterophilic ligands will preferentially interact with L1 in its resting conformation.

The integrin $\alpha_9\beta_1$ identified as an L1 binding partner in this study has a limited tissue distribution that includes epithelia, muscle, and cells of the myelomonocytic series (Palmer et al., 1993; Taooka et al., 1999); no expression has been reported in the nervous system. The $\alpha_9\beta_1$ integrin is also present on melanoma cells (Smith and Giachelli, 1998) and a variety of carcinoma cell lines (Palmer et al., 1993), suggesting a potential role in tumor development. An overlap in expression between L1 and $\alpha_9\beta_1$ is expected since L1 also has been described on a variety of epithelial structures (Thor et al., 1987; Debiec et al., 1998; Kujat et al., 1995), on carcinoma and melanoma cell lines, and on normal and transformed myelomonocytic cells (Mujoo et al., 1986; Linnemann et al., 1989; Reid and Hemperly, 1992; Pancook et al., 1997). Recently, it has been demonstrated that $\alpha_9\beta_1$ can promote neutrophil transendothelial cell migration via an interaction with VCAM-1 (Taooka et al., 1999). L1–$\alpha_9\beta_1$ interactions may also modulate transendothelial cell migration either directly by promoting adhesion to the endothelium or indirectly by modulating the activity of $\alpha_9\beta_1$ and its ability to bind to VCAM-1. Similarly, the $\beta_1$-mediated adhesion of eosinophils to endothelial cells has also been shown to be modulated by ligation of PECAM-1 on endothelial cells (Chiba et al., 1999). In this regard, L1 has not only been described on myelomonocytic cells and metastatic tumor lines (Mujoo et al., 1986; Linnemann et al., 1989; Reid and Hemperly,

1992; Pancook et al., 1997), but also on activated small vessel endothelium in certain diseases (Felding-Habermann et al., 1997).

The observation that the integrins identified in this study are interacting with multimeric FN3 is consistent with the concept that L1 clustering is important for the recruitment of integrins, and would also explain why $\alpha_9\beta_1$ can only be colocalized with L1 at cell–cell interfaces, where classical L1–L1 homophilic interactions and consequent clustering would be expected to occur. The concept that ligand polymerization can potentiate integrin binding is supported by recent work that demonstrates preferential integrin-mediated adhesion to multivalent, rather than monovalent extracellular matrix components in lymphoid cells (Stupak et al., 1999). Indeed, a primary regulator of inflammatory cell entry into sites of wounding is the accumulation of polymerized provisional matrix components including fibrin, fibronectin, and vitronectin (Dvorak et al., 1995). Although the enhanced affinity of the aforementioned matrices primarily rely upon appropriate spacing or exposure of canonical cell adhesion motifs (e.g., RGD), it is not clear whether the integrin–L1 interactions described in this report are due to the creation of neorecognition sites within the complexed ligand, or rather reflect the optimal presentation of multiple, appropriately spaced, previously available, low affinity binding motifs in such a manner that the clustered motifs stabilize integrin binding through avidity modulation.

An important implication of the work presented here is that cell–cell contact and concomitant L1 clustering can potentiate integrin activation and/or signaling. As a consequence, L1 may directly modulate those processes normally associated with integrin-binding to the extracellular matrix, including cell motility, survival, and proliferation. The fact that $\alpha_v\beta_3$ can associate with L1 via interaction with its RGD motif (Montgomery et al., 1996; Felding-Habermann et al., 1997; Oleszewski et al., 1999) as well as via an interaction with the multimerized FN3 domain suggests an interdependent relationship that may have important ramifications for cell survival and motility. For example, a recent study has shown that $\alpha_v\beta_3$ is essential for the survival of melanoma cells in the dermal microenvironment, however, detailed examination of these cells indicates that they are surviving as cell clusters (Hsu et al., 1998). In this context cell–cell interaction and concomitant L1–$\alpha_v\beta_3$ ligation may represent an important survival mechanism. The ability of L1 to induce signaling via its interaction with integrins requires confirmation, however, the early steps of neurite extension on L1 are dependent on protein phosphorylation events involving the nonreceptor tyrosine kinase pp60c-src, a known mediator of integrin signaling (Ignelzi et al., 1994), suggesting that L1 interactions may indeed facilitate signaling in this manner.

The findings reported here significantly extend our current knowledge of L1–integrin interactions. We have documented two novel integrin-binding sequences within putative loops in the third FN-like domain of L1. One of these sequences is shown to self-associate, resulting in both domain multimerization and integrin ligation. To our knowledge, this is the first report of a spontaneously self-associating peptide sequence that can also support direct integrin binding. Dual regulation of FN3-integrin binding is proposed based on conformational constraints and sensitivity to proteolysis. Based on our observations, and those of others, we propose a model in which distal transligation of L1 at the cell–cell interface induces a conformation change within the L1 ectodomain that culminates in receptor multimerization and integrin recruitment via the FN3 domain. The findings presented in this study further suggest an intimate association between integrins and L1, an association that may have important implications for downstream signaling events.

This study was supported by the National Cancer Institute (NCI) RO1 grant CA69112-01 and by National Heart, Lung and Blood Institute (NHLB) RO1 grant HL62477-01 (to A.M.P. Montgomery) and by the NCI research fellowship (S. Silletti) 1F32 CA72192-01. This is Scripps manuscript #12868-IMM.

Submitted: 13 December 1999
Revised: 1 May 2000
Accepted: 23 May 2000

*Note Added in Proof.* While this manucript was being reviewed, it was reported that the third fibronectin repeat of L1 is required for L1 to serve as an optimal substratum for neurite extension. Stallcup, W.B. 2000. *J. Neurosci. Res.* 61:33–43.

*References*

Appel, F., J. Holm, J.-F. Conscience, and M. Schachner. 1993. Several extracellular domains of the neural cell adhesion molecule L1 are involved in neurite outgrowth and cell body adhesion. *J. Neurosci.* 13:4764–4775.

Appel, F., J. Holm, J.-F. Conscience, F. von Bohlen und Halbach, A. Faissner, P. James, and M. Schachner. 1995. Identification of the border between fibronectin type III homologous repeats 2 and 3 of the neural cell adhesion molecule L1 as a neurite outgrowth promoting and signal transducing domain. *J. Neurobiol.* 28:297–312.

Bastmeyer, M., H. Ott, C.A. Leppert, and C.A. Stuermer. 1995. Fish E587 glycoprotein, a member of the L1 family of cell adhesion molecules participates in axonal fasciculation and the age-related order of ganglion cell axons in goldfish retina. *J. Cell Biol.* 130:969–976.

Bateman, A., M. Jouet, J. MacFarlane, J.-S. Du, S. Kenwrick, and C. Chothia. 1996. Outline structure of the human L1 cell adhesion molecule and the sites where mutations cause neurological disorders. *EMBO (Eur. Mol. Biol. Organ.) J.* 15:6050–6059.

Berditchevski, F., and E. Odintsova. 1999. Characterization of integrin-tetraspanin adhesion complexes: role of tetraspanins in integrin signaling. *J. Cell Biol.* 146:477–492.

Bieber, A.J., P.M. Snow, M. Hortsch, N.H. Patel, J.R. Jacobs, Z.R. Traquina, J. Schilling, and C.S. Goodman. 1989. *Drosophila* neuroglian: a member of the immunoglobulin superfamily with extensive homology to the vertebrate neural cell adhesion molecule L1. *Cell.* 59:447–460.

Bock, E.C., C. Richter-Landsberg, A. Faissner, and M. Schachner. 1985. Demonstration of immunochemical identity between the nerve growth factor-inducible large external (NILE) glycoprotein and the cell adhesion molecule L1. *EMBO (Eur. Mol. Biol. Organ.) J.* 4:2765–2768.

Brummendorf, T., S. Kenwick, and F.G. Rathjen. 1998. Neural recognition molecule L1: from cell biology to human hereditary brain malformations. *Curr. Opin. Neurobiol.* 8:87–97.

Burgoon, M.P., R.B. Hazan, G.R. Phillips, K.L. Crossin, G.M. Edelman, and B.A. Cunningham. 1995. Functional analysis of posttranslational cleavage products of the neuron–glia cell adhesion molecule Ng-CAM. *J. Cell Biol.* 130:733–744.

Chiba, R., N. Nakagawa, K. Kurasawa, Y. Tanaka, Y. Saito, and I. Iwamoto. 1999. Ligation of CD31 (PECAM-1) on endothelial cells increases adhesive function of $\alpha_v\beta_3$ integrin and enhances $\beta_1$ integrin-mediated adhesion of eosinophils to endothelial cells. *Blood.* 94:1319–1329.

Cohen, N.R., J.S.H. Taylor, L.B. Scott, R.W. Guillery, P. Soriano, and A.J. Furley. 1997. Errors in corticospinal axon guidance in mice lacking the neural cell adhesion molecule L1. *Curr. Biol.* 8:26–33.

Dahme, M., U. Bartsch, R. Martini, B. Anliker, M. Schachner, and N. Mantei. 1997. Disruption of the gene coding for the cell adhesion molecule L1 leads to malformations of the nervous system in mice. *Nat. Genet.* 17:346–349.

Debiec, H., E.I. Christensen, and P.M. Ronco. 1998. The cell adhesion molecule L1 is developmentally regulated in the renal epithelium and is involved in kidney branching morphogenesis. *J. Cell Biol.* 143:2067–2079.

Demyanenko, G.P., A.Y. Tsai, and P.F. Maness. 1999. Abnormalities in neuronal process extension, hippocampal development, and the ventricular system of L1 knockout mice. *J. Neurosci.* 19:4907–4920.

Di Sciullo, G., T. Donahue, M. Schachner, and S.A. Bogen. 1998. L1 antibodies

block lymph node fibroblastic reticular matrix remodeling in vivo. *J. Exp. Med.* 187:1953–1963.

Drescher, B., E. Spiess, M. Schachner, and R. Probstmeier. 1996. Structural analysis of the murine cell adhesion molecule L1 by electron microscopy and computer-assisted modelling. *Eur. J. Neurosci.* 8:2467–2478.

Dvorak, H.F., L.F. Brown, M. Detmar, and A.M. Dvorak. 1995. Vascular permeability factor/vascular endothelial growth factor, microvascular hyperpermeability, and angiogenesis. *Am. J. Pathol.* 146:1029–1039.

Ebeling, O., A. Duczmal, S. Aigner, C. Geiger, S. Schollhammer, J.T. Kemshead, P. Moller, R. Schwartz-Albiez, and P. Altevogt. 1996. L1 adhesion molecule on human lymphocytes and monocytes: expression and involvement in binding to $\alpha_v\beta_3$ integrin. *Eur. J. Immunol.* 26:2508–2516.

Faissner, A., D.B. Teplow, D. Kübler, G. Keilhauer, V. Kinzel, and M. Schachner. 1985. Biosynthesis and membrane topography of the neural cell adhesion molecule L1. *EMBO (Eur. Mol. Biol. Organ.) J.* 4:3105–3113.

Feizi, A. 1994. Evidence for carbohydrate-mediated interactions between the neural-cell-adhesion molecules NCAM and L1. *Trends Biochem. Sci.* 19: 233–234.

Felding-Habermann, B., S. Silletti, F. Mei, C.-H. Siu, P. Yip, P.C. Brooks, D.A. Cheresh, T.E. O'Toole, M.H. Ginsberg, and A.M.P. Montgomery. 1997. A single immunoglobulin-like domain of the human neural adhesion molecule L1 supports adhesion by multiple vascular and platelet integrins. *J. Cell Biol.* 139:1567–1581.

Felsenfeld, D.P., M.A. Hynes, K.M. Skoler, A.J. Furley, and T.M. Jessell. 1994. TAG-1 can mediate homophilic binding, but neurite outgrowth on TAG-1 requires an L1-like molecule and $\beta_1$ integrins. *Neuron.* 12:675–690.

Fransen, E., G.V. Camp, L. Vits, and P.J. Willems. 1997. L1-associated diseases: clinical geneticists divide, molecular geneticists unite. *Hum. Mol. Genet.* 6:1625–1632.

Haney, C.A., Z. Sahenk, C. Li, V.P. Lemmon, J. Roder, and B.D. Trapp. 1999. Heterophilic binding of L1 on unmyelinated sensory axons mediates Schwann cell adhesion and is required for axonal survival. *J. Cell Biol.* 1463: 1173–1183.

Holm, J., F. Appel, and M. Schachner. 1995. Several extracellular domains of the neural cell adhesion molecule L1 are involved in homophilic interactions. *J. Neurosci. Res.* 42:9–20.

Hortsch, M. 1996. The L1 family of neural cell adhesion molecules: old proteins performing new tricks. *Neuron.* 17:587–593.

Hsu, M.Y., D.T. Shih, F.E. Meier, P. Van Belle, J.Y. Hsu, D.E. Elder, C.A. Buck, and M. Herlyn. 1998. Adenoviral gene transfer of β3 integrin subunit induces conversion from radial to vertical growth phase in primary melanoma. *Am. J. Pathol.* 153:1435–1442.

Ignelzi, M.A., D.R. Miller, P. Soriano, and P.F. Maness. 1994. Impaired neurite outgrowth of src-minus cerebellar neurons on the cell adhesion molecule L1. *Neuron.* 12:873–884.

Jung, M., B. Petrausch, and C.A.O. Stuermer. 1997. Axon-regenerating retinal ganglion cells in adult rats synthesize the cell adhesion molecule L1 but not TAG-1 or SC-1. *Mol. Cell. Neurosci.* 9:116–131.

Kadmon, G., A.B. Imhof, P. Altevogt, and M. Schachner. 1995. Adhesive hierarchy involving the cell adhesion molecules L1, CD24, and α6 integrin in murine neuroblastoma N2A cells. *Biochem. Biophys. Res. Commun.* 214:94–101.

Katayama, M., A. Iwamatsu, H. Mastani, K. Furuke, K. Takeda, H. Wada, T. Masuda, and K. Ishii. 1997. Expression of neural cell adhesion molecule L1 in human lung. *Cell Struct. Funct.* 22:511–516.

Krystosek, A., and N.W. Seeds. 1981. Plasminogen activator release at the neuronal growth cone. *Science.* 213:1532–1534.

Kujat, R., F. Miragall, D. Krause, R. Dermietzel, and K.H. Wrobel. 1995. Immunolocalization of the neural cell adhesion molecule L1 in non-proliferating epithelial cells of the male urogenital tract. *Histochem. Cell Biol.* 103: 311–321.

Kunz, S., M. Spirig, C. Ginsberg, A. Buchstaller, P. Berger, R. Lanz, C. Rader, L. Vogt, B. Kunz, and P. Sonderegger. 1998. Neurite fasciculation mediated by complexes of axonin-1 and Ng cell adhesion molecule. *J. Cell Biol.* 143: 1673–1690.

Lagenaur, C., and V. Lemmon. 1987. An L1-like molecule, the 8D9 antigen, is a potent substrate for neurite extension. *Proc. Natl. Acad. Sci. USA.* 84:7753–7757.

Lemmon, V., and S.C. McLoon. 1986. The appearence of an L1-like molecule in the chick visual pathway. *J. Neurosci.* 6:2987–2994.

Lindner, J., F.G. Rathjen, and M. Schachner. 1983. L1 mono- and polyclonal antibodies modify cell migration in early postnatal mouse cerebellum. *Nature.* 305:427–430.

Linnemann, D., A. Raz, and E. Bock. 1989. Differential expression of cell adhesion molecules in variants of the K1735 melanoma cells differing in metastatic capacity. *Int. J. Cancer.* 43:709–712.

Luthl, A., J.-P. Laurent, A. Figurov, D. Muller, and M. Schachner. 1994. Hippocampal long term potentiation and neural cell adhesion molecules L1 and NCAM. *Nature.* 372:777–779.

Martini, R., and M. Schachner. 1986. Immunoelectron microscopic localization of neural cell adhesion molecules (L-1, N-CAM, and MAG) and their shared carbohydrate epitope and myelin basic protein in developing sciatic nerve. *J. Cell Biol.* 103:2439–2448.

Mizutani, A., H. Saito, and N. Matsuki. 1996. Possible involvement of plasmin in long term potentiation of rat hippocampal slices. *Brain Res.* 739:276–281.

Montgomery, A.M.P., J.C. Becker, C.-H. Siu, V. Lemmon, D.A. Cheresh, J.D. Pancook, X. Zhoa, and R.A. Reisfeld. 1996. Human neural cell adhesion molecule L1 and rat homologue NILE are ligands for integrin $\alpha_v\beta_3$. *J. Cell Biol.* 132:475–485.

Moos, M., R. Tacke, H. Scherer, D. Teplow, K. Fruh, and M. Schachner. 1988. Neural adhesion molecule L1 as a member of the immunoglobulin superfamily with binding domains similar to fibronectin. *Nature.* 334:701–703.

Mujoo, K., R.C. Spiro, and R.A. Reisfeld. 1986. Characterization of a unique glycoprotein antigen expressed on the surface of human neuroblastoma cells. *J. Biol. Chem.* 261:10299–10309.

Nayeem, N., S. Silletti, X.-M. Yang, V.P. Lemmon, R.A. Reisfeld, W.B. Stallcup, and A.M.P. Montgomery. 1999. A potential role for the plasmin(ogen) system in the posttranslational cleavage of the neural cell adhesion molecule L1. *J. Cell Sci.* 112:4739–4749.

Nybroe, O., A.M. Dalseg, and E. Bock. 1990. A developmental study of soluble L1. *Int. J. Dev. Neurosci.* 8:273–281.

Ohnishi, T., H. Matsumura, S. Izumoto, S. Hiraga, and T. Hayakawa. 1998. A novel model of glioma cell invasion using organotypic brain slice culture. *Cancer Res.* 58:2935–2940.

Oleszewski, M., S. Beer, S. Katich, C. Geiger, Y. Zeller, U. Rauch, and P. Altevogt. 1999. Integrin and neurocan binding to L1 involves distinct Ig domains. *J. Biol. Chem.* 274:24602–24610.

Palmer, E.L., C. Ruegg, R. Ferrando, R. Pytela, and D. Sheppard. 1993. Sequence and tissue distribution of the integrin $\alpha_9\beta_1$ subunit, a novel partner of $\beta_1$ that is widely distributed in epithelia and muscle. *J. Cell Biol.* 123:1289–1297.

Pancook, J.D., R.A. Reisfeld, N. Varki, A. Vitiello, R.I. Fox, and A.M.P. Montgomery. 1997. Expression and regulation of the neural cell adhesion molecule L1 on human cells of myelomonocytic and lymphoid origin. *J. Immunol.* 158:4413–4421.

Porter, J.C., and N. Hogg. 1998. Integrins take partners: cross-talk between integrins and other membrane receptors. *Trends Cell Biol.* 8:390–396.

Rathjen, F.G., and M. Schachner. 1984. Immunocytological and biochemical characterization of a new neuronal cell surface component (L1 antigen) which is involved in cell adhesion. *EMBO (Eur. Mol. Biol. Organ.) J.* 3:1–10.

Reid, R.A., and J.J. Hemperly. 1992. Variants of human L1 cell adhesion molecule arise through alternate splicing of RNA. *J. Mol. Neurosci.* 3:127–135.

Sadoul, K., R. Sadoul, A. Faissner, and M. Schachner. 1988. Biochemical characterization of different molecular forms of the neural cell adhesion molecule L1. *J. Neurochem.* 50:510–521.

Salles, F.J., N. Schechter, and S. Strickland. 1990. A plasminogen activator is induced during goldfish optic nerve regeneration. *EMBO (Eur. Mol. Biol. Organ.) J.* 9:2471–2477.

Schmidt, C., V. Kunemund, E.S. Wintergerst, B. Schmitz, and M. Schachner. 1996. CD9 of mouse brain is implicated in neurite outgrowth and cell migration in vitro and is associated with the $\alpha_6\beta_1$ integrin and the neural adhesion molecule L1. *J. Neurosci. Res.* 43:12–31.

Seeds, N.W., L.B. Siconolfi, and S.P. Haffke. 1997. Neuronal extracellular proteases facilitate cell migration, axonal growth, and pathfinding. *Cell Tissue Res.* 290:367–370.

Smith, L.L., and C.M. Giachelli. 1998. Structural requirements for $\alpha_9\beta_1$-mediated adhesion and migration to thrombin-cleaved osteopontin. *Exp. Cell Res.* 242:351–360.

Stupak, D.G., E. Li, S.A. Silletti, J.A. Kehler, R.L. Geahlen, K. Hahn, G.R. Nemerow, and D.A. Cheresh. 1999. Matrix valency regulates integrin-mediated lymphoid adhesion via syk kinase. *J. Cell Biol.* 144:777–787.

Su, X.-D., L.N. Gastinel, D.E. Vaughn, I. Faye, P. Poon, and P.J. Bjorkman. 1998. Crystal structure of hemolin: a horseshoe shape with implications for homophilic adhesion. *Science.* 281:991–995.

Taooka, Y., J. Chen, T. Yednock, and D. Sheppard. 1999. The integrin $\alpha_9\beta_1$ mediates adhesion to activated endothelial cells and transendothelial neutrophil migration through interaction with vascular cell adhesion molecule 1. *J. Cell Biol.* 145:413–420.

Thor, G., R. Probstmeier, and M. Schachner. 1987. Characterization of the cell adhesion molecules L1, N-CAM and J1 in the mouse intestine. *EMBO (Eur. Mol. Biol. Organ.) J.* 6:2581–2586.

Tongiorgi, E., R.R. Bernhardt, and M. Schachner. 1995. Zebrafish neurons express two L1-related molecules during early axonogenesis. *J. Neurosci. Res.* 42:547–561.

Viollet, C., and P. Doherty. 1997. CAMs and the FGF receptor: an interacting role in axonal growth. *Cell Tissue Res.* 290:451–455.

Wolff, J.M., R. Frank, K. Mujoo, R. Spiro, R.A. Reisfeld, and F.G. Rathjen. 1988. A human brain glycoprotein related to the mouse cell adhesion molecule L1. *J. Biol. Chem.* 263:11943–11947.